Molecular and Supramolecular Synthesis with Dibenzofuran-Containing Systems[**]

Masumi Asakawa, Peter R. Ashton, Christopher L. Brown, Matthew C. T. Fyfe, Stephan Menzer, Dario Pasini, Cecile Scheuer, Neil Spencer, J. Fraser Stoddart,[*] Andrew J. P. White, and David J. Williams

Abstract: The template-directed syntheses of two new tetracationic cyclophanes, cyclobis(paraquat-2,8-dibenzofuran) and cyclobis(paraquat-3,7-dibenzofuran), incorporating dibenzofuran subunits has been accomplished. Initially, the cyclophanes were self-assembled around a macrocyclic polyether template, bis-*p*-phenylene[34]crown-10 (BPP34C10), to form catenanes: the mechanical bond order of the catenane formed determined the requisite "amacrocyclic" templates for synthesis of the free cyclophane. X-ray crystallography shows that both of the cyclophanes possess rectangular covalent frameworks. Furthermore, these cyclophanes form self-assembled tapes in the solid state, since the dibenzofuran moieties have a tendency to associate with each other through crossed $\pi-\pi$ stacks. The dibenzofuran-containing catenanes also form two-dimensional supramolecular arrays in the solid state on account of extended $\pi-\pi$ stacking interactions. In addition, the serendipitous discovery of a plerotopic tecton (consisting of a dibenzofuran nucleus covalently linked from the 2- and 8-positions by methylene groups to 4,4′-pyridylpyridinium (hydrogen bond acceptor) and protonated bipyridinium (hydrogen bond donor) units) has been made. The tecton dimerizes in the solid state to form a supramolecular macrocycle, since its complementary hydrogen bonding sites are oriented in a horseshoe-like fashion by the 2,8-disubstituted dibenzofuran unit. However, this superstructure is not retained in the 1:1 complex of the tecton with BPP34C10: cocrystallization of the tecton with this crown ether opens the macrocyclic two-component supermolecule to afford a hydrogen-bonded pseudopolyrotaxane.

Keywords
crystal engineering · dibenzofuran · molecular quadrilaterals · supramolecular chemistry · template synthesis

Introduction

In recent years, supramolecular chemistry—the chemistry of the noncovalent bond—has become a rapidly developing field of contemporary science.[1] Its evolution is limited only by the creativity of the chemists who fashion the superstructures for its two subfamilies, 1) the oligo(supra)molecular *supermolecules*,[2] whose discrete supramolecular structure is defined by the noncovalent association of a finite number of supramolecular building blocks, and 2) the infinite, poly(supra)molecular *supramolecular arrays*[3] formed by the noncovalent combination of a multitudinous, unspecified number of tectons.[4] Solid-state supramolecular chemistry, that is, crystal engineering,[5] is an emerging domain within the realm of supramolecular chemistry; it seeks to rationalize the noncovalent forces that determine the packing of a particular crystal to form specific supramolecular aggregates or arrays, with a view to the creation of new supramolecular materials,[6] namely, functioning, organized nanostructures.[7] Many of the intermolecular bonding tools available to the supramolecular scientist have been used for the noncovalent synthesis of polymeric supramolecular arrays by self-assembly.[8] In particular, hydrogen bonds,[9] coordinate covalent bonds formed between metals and ligands,[10] $\pi-\pi$ stacking interactions,[11] heteroatom–halogen interactions,[12] or combinations of these noncovalent interactions[13] have all been used as the supramolecular "adhesive" that holds the solid-state supramolecular polymer together.

A recent report from our laboratories describes the solid-state supramolecular synthesis of mosaics and nanotubes employing the plerotopic (self-complementary) cyclophane $\mathbf{1}^{4+}$ (Scheme 1).[14] The cyclophane has π-electron-rich and π-elec-

---

[*] Prof. J. F. Stoddart, Dr. M. Asakawa, Dr. C. L. Brown, Dr. N. Spencer, P. R. Ashton, M. C. T. Fyfe, D. Pasini
School of Chemistry, University of Birmingham
Edgbaston, Birmingham B15 2TT (UK)
Fax: Int. code +(121)414-3531
e-mail: j.f.stoddart@bham.ac.uk
Prof. D. J. Williams, Dr. S. Menzer, Dr. A. J. P. White, C. Scheuer
Department of Chemistry, Imperial College
South Kensington, London SW7 2AY (UK)
Fax: Int. code +(171)594-5804

[**] Molecular Meccano, Part 18; for Part 17, see D. B. Amabilino, P. R. Ashton, S. E. Boyd, M. Gómez-López, W. Hayes, J. F. Stoddart, *J. Org. Chem.* **1997**, *62*, 3062–3075.

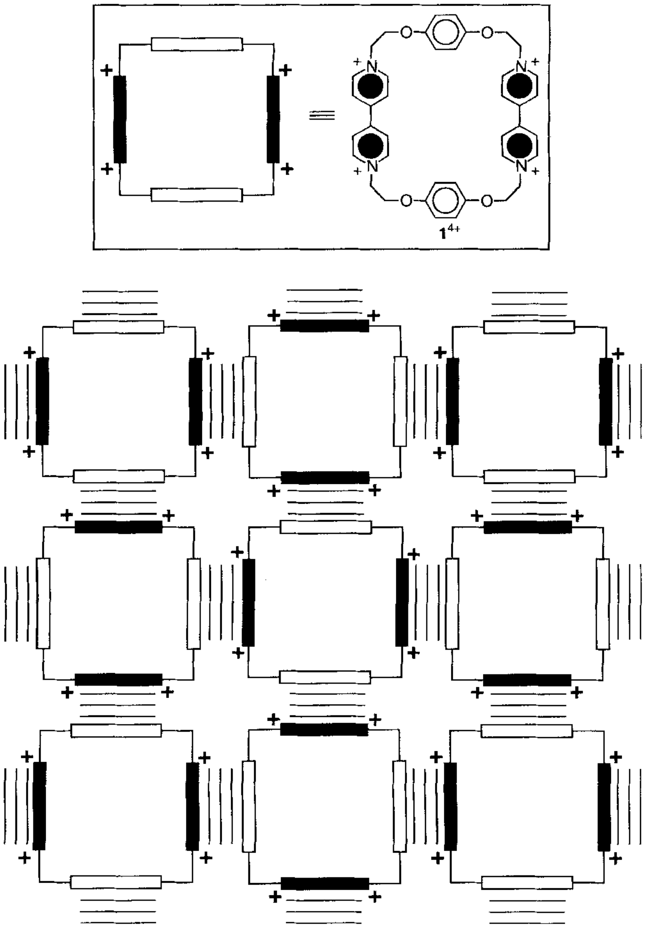

Scheme 1. Schematic representation of the two-dimensional mosaic formed by the noncovalent polymerization of the 1^{4+} cyclophane.

tron-deficient subunits alternating around its macrocyclic periphery and acts as an endoreceptor. Complementary hydroquinone and bipyridinium units π–π stack with each other to form a highly structured supramolecular polymer (specifically, a mosaic) in two dimensions, while channels reminiscent of nanotubes are formed in the third dimension. Furthermore, we have recently outlined a practical synthesis of the organic molecular square cyclobis(paraquat-4,4′-biphenylene) 2^{4+} on a preparative scale.[15] The isolation of this tetracationic cyclophane in reasonable yield has permitted an examination of its X-ray crystal structure. Once again, the formation of a supramolecular polymer in the solid state is observed: partial and complete π–π stacking for the biphenylene and bipyridinium units, respectively, of this tetracationic cyclophane leads to a mosaic-like supramolecular array. Against this background, we decided to combine both of the features of these two systems, and designed organic molecular quadrilaterals in which π-electron-rich and π-electron-poor subunits alternate around the periphery of the tetracationic cyclophane.[16] The tectons we have prepared contain the dibenzofuran[17,18] and 4,4′-bipyridinium[19] (also termed viologen or paraquat) subunits. We expected that the incorporation of the dibenzofuran unit would facilitate the covalent synthesis of the new tetracationic macrocycles. Their requisite dihalide precursors are benzylic; thus the rate of formation of the organic molecular quadrilaterals is increased. This contrasts with the cyclophane 1^{4+}, preparation of which gives a low yield (12%) and requires the use of ultra-high pressure (12 kbar).[14] Furthermore, we hoped that the addition of the dibenzofuran moiety to the tetracationic cyclophanes (Figure 1) would add another dimension to our endeavors in solid-state supramolecular synthesis, perhaps yielding π-stacked two-dimensional arrays and nanotubes, analogous to the related cyclophane 1^{4+}.[14]

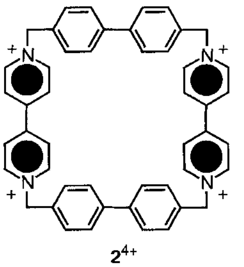

2^{4+}

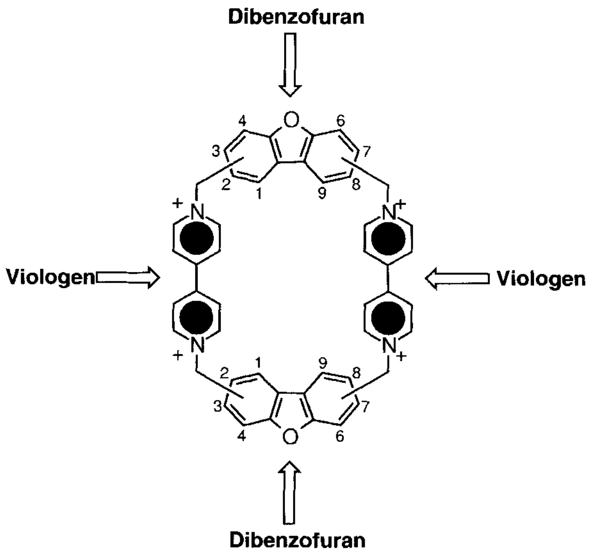

Figure 1. Organic molecular quadrilaterals containing dibenzofuran and 4,4′-bipyridinium subunits.

Results and Discussion

Molecular Synthesis: We have employed a synthetic strategy involving 1) the initial preparation (using the supramolecular assistance to synthesis provided by a variety of noncovalent forces,[8f, 20] especially π–π stacking interactions) of the tetracationic cyclophanes around a macrocyclic polyether template leading to catenanes,[21] followed by 2) examination of the mechanical bond order of the catenane formed, so that the appropriate "amacrocyclic" template[22] for the synthesis of the non-interlocked, "free" tetracationic cyclophanes can be determined.[15]

2,8-Disubstitution on the Dibenzofuran Subunit: Synthesis of the [2]Catenane 5·4 PF_6 and the Tetracationic Cyclophane 6·4 PF_6: Reaction of an excess of 4,4′-bipyridine with 2,8-bis(chloromethyl)dibenzofuran 3[23] in refluxing MeCN gave the dicationic salt[24] 4·2 PF_6 in 43% yield after counterion exchange with dry NH_4PF_6. The salt 4·2 PF_6 was then allowed to react with a slight excess of dichloride 3 in the presence of the macrocyclic polyether bis-*p*-phenylene[34]crown-10 (BPP34C10)[25,26] and a catalytic amount of NaI in MeCN at 20 °C for 19 d to give the dibenzofuran-containing [2]catenane 5·4 PF_6 in 30% yield after column chromatography and counterion exchange (Scheme 2).[27,28] The isolation of no catenanes with a higher

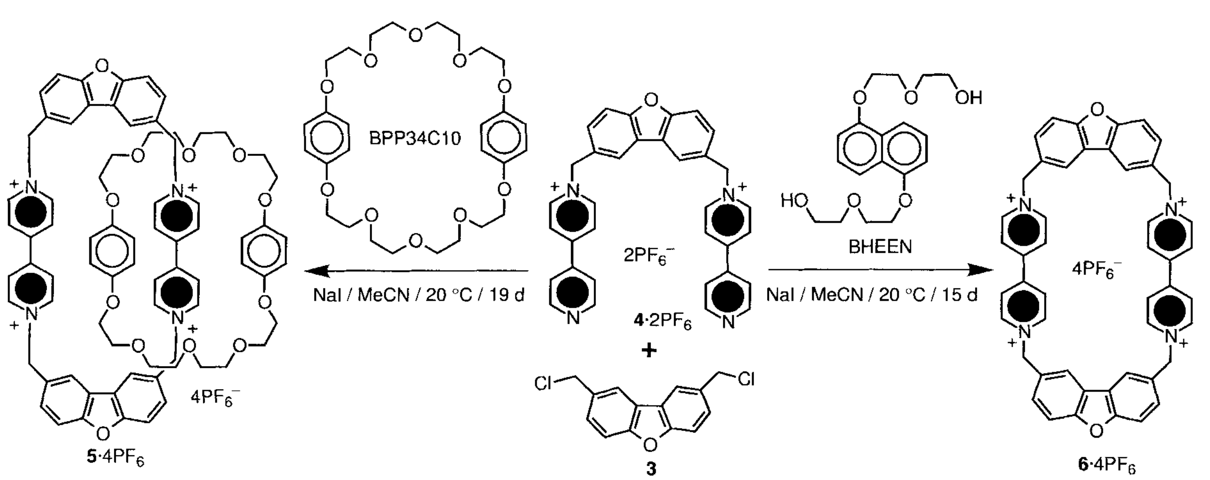

Scheme 2. Synthesis of the [2]catenane $5\cdot4PF_6$ and the tetracationic cyclophane $6\cdot4PF_6$.

mechanical bond order from this reaction suggested to us that a suitable π-electron-rich arene such as 1,5-bis[2-(2-hydroxyethoxy)ethoxy]naphthalene[29] (BHEEN) would act as a template for the formation of the uncatenated cyclophane.[30] Indeed, reaction of the bis(hexafluorophosphate) salt $4\cdot2PF_6$ and the dichloride **3** in the presence of BHEEN and a catalytic amount of NaI in MeCN at ambient temperature/pressure for 15 d gave the free tetracationic cyclophane $6\cdot4PF_6$ in 49% yield after anion exchange. However, the template effect of the π-electron-rich arene is modest, since the tetracationic cyclophane was obtained in 40% yield in the absence of BHEEN under analogous reaction conditions, suggesting that the reactive pyridyl sites are juxtaposed in an orientation favorable for the closure of the macroring on reaction with the dichloride **3**; that is, the "stiffening" effect of the dibenzofuran moiety encourages the macrocyclization by reducing the entropy cost of the final ring closure.

Serendipity has played an important role in the development of supramolecular chemistry,[31] beginning with Pedersen's discovery of the crown ethers[32] and continuing up to contemporary catenane syntheses.[33] In our earliest preparations of the dicationic salt $4\cdot2PF_6$ we discovered a novel compound by chance when $4\cdot2Cl$ was treated with an aqueous solution of practical grade NH_4PF_6. This novel compound gave a deep red solution, suggestive of charge transfer interactions, when mixed with BPP34C10 in MeCN or Me_2CO, and was bound by this macrocyclic polyether with a high association constant (vide infra). Neither 5^{4+} nor 6^{4+} was produced when the novel compound was treated with the dichloride **3**, in the presence or absence of BPP34C10, in MeCN for 6 weeks at 20 °C. Despite some chemical shift differences, the compound has a similar ^1H NMR spectrum to that of $4\cdot2PF_6$, the protons on the benzyl rings of the dibenzofuran unit and the protons on the bipyridinium unit apparently being equivalent. Unlike $4\cdot2PF_6$, the compound did not decompose on heating. Analysis showed it to be $[4\cdot2PF_6 + HPF_6]$, and the structure was shown by X-ray crystallography (vide infra) to be $4{-}H\cdot3PF_6$, consisting of a central dibenzofuran nucleus covalently linked to 4,4′-pyridylpyridinium and protonated bipyridinium units by methylene bridges.

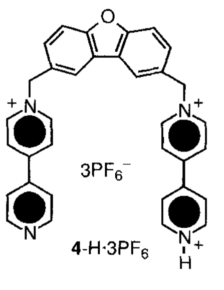

$4\text{-}H\cdot3PF_6$

3,7-Disubstitution on the Dibenzofuran Subunit–Synthesis of the [3]Catenane $9\cdot4PF_6$ and the Tetracationic Cyclophane $10\cdot4PF_6$: The 3,7-disubstituted analogue of $4\cdot2PF_6$, namely $8\cdot2PF_6$, was readily acquired in 86% yield from the reaction of 3,7-bis(bromomethyl)dibenzofuran **7**[34] with a surplus of 4,4′-bipyridine, followed by counterion exchange (Scheme 3). Reaction of this dicationic salt with the dibromide **7** in the presence of BPP34C10 furnished the [3]catenane[35,36] $9\cdot4PF_6$ in 18% yield after column chromatography and counterion exchange. The formation of the [3]catenane implied that, like cyclobis(paraquat-4,4′-biphenylene) (2^{4+}),[15] ferrocene ($FeCp_2$) and its derivatives should be effective templates for the synthesis of the corresponding "free" tetracationic cyclophane $10\cdot4PF_6$, since their π-electron-rich cyclopentadienyl rings can associate with the π-electron-deficient bipyridinium units of the intermediates by π–π stacking interactions. In fact, the tetracationic cyclophane $10\cdot4PF_6$ is obtained in a remarkable 37% yield (after counterion exchange) when the dibromide **7** reacts with the dicationic salt $8\cdot2PF_6$ in the presence of 22 molar equivalents of $FeCp_2$ in MeCN/DMF at 20 °C for 17.5 days. In contrast, the yield of the tetracationic cyclophane was a meager 6% when the reaction was carried out in the absence of $FeCp_2$ under otherwise identical conditions. We believe that the increased efficiency of both the template-directed and template-free syntheses of the 10^{4+} cyclophane (cf. the isolated yields for $2\cdot4PF_6$ are 10% and 2% for the $FeCp_2$-present and $FeCp_2$-free preparations, respectively[15]) can be attributed to the loss of the rotation about the bond joining the two benzene rings of the rigidly fixed, fused polyaromatic dibenzofuran system. This moiety holds the reactive nucleophilic and electrophilic sites within the acyclic tricationic intermediate in a relatively rigid orientation, where they are more predisposed to form the tetracationic macrocycle.

Association Constants: We have evaluated the association constants (K_a) of the tetracationic cyclophanes with the templates used for their synthesis in order that we might obtain a correlation between the yields of the template-free and template-direct-

0947-6539/97/0307-1138 $ 17.50+.50/0

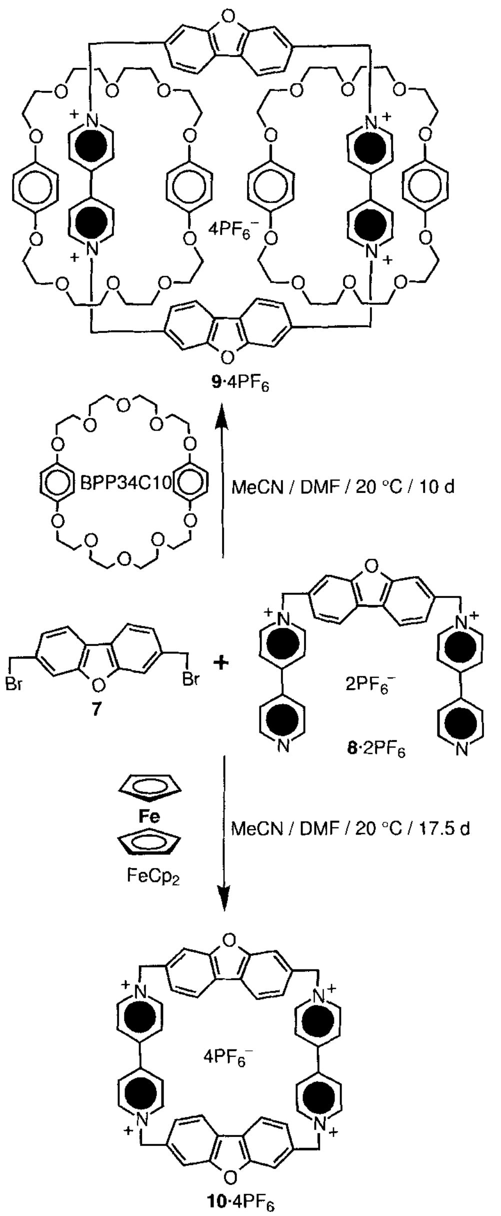

Scheme 3. Synthesis of the [3]catenane $\mathbf{9}\cdot 4PF_6$ and the tetracationic cyclophane $\mathbf{10}\cdot 4PF_6$.

Table 1. Association constants (K_a) and derived free energies of complexation ($-\Delta G^\circ$) for the $[\mathbf{6}\cdot \mathrm{BHEEN}]^{4+}$ and $[\mathbf{10}\cdot \mathrm{FeCp_2}]^{4+}$ complexes in MeCN at 298 K, and for the $[\mathbf{4}-\mathrm{H}\cdot \mathrm{BPP34C10}]^{3+}$ complex in Me_2CO at 298 K.

Complex	K_a (M^{-1})	$-\Delta G^\circ$ (kcal mol^{-1})	λ_{max} [c] (nm)
$[\mathbf{6}\cdot\mathrm{BHEEN}][PF_6]_4$ [a]	17	1.7	433
$[\mathbf{10}\cdot\mathrm{FeCp_2}][PF_6]_4$ [b]	38	2.2	–
$[\mathbf{4}-\mathrm{H}\cdot\mathrm{BPP34C10}][PF_6]_3$ [a]	1190	4.2	433

[a] The association constants were evaluated by UV/Vis spectroscopy by means of the titration methodology (ref. [37]). [b] The stability constant was measured by ^{1}H NMR spectroscopy with the titration method (refs. [37,38]). The protons on the tetracationic cyclophane situated in the β position with respect to the bipyridinium nitrogen atoms were used as the probe nuclei. [c] Wavelength corresponding to the maximum of the charge-transfer band originating from the interaction between the viologen unit and the hydroquinone or 1,5-dioxynaphthalene ring systems.

ed preparations and the stability constants of the complexes (Table 1). Solutions containing equimolar quantities of BHEEN and $\mathbf{6}\cdot 4PF_6$ in MeCN are very pale pink, qualitatively indicating a low stability constant for the $[\mathbf{6}\cdot\mathrm{BHEEN}]^{4+}$ complex. The modest association constant calculated for this complex (Table 1) compares well with the relative inactivity of the BHEEN molecule to act as a template for the synthesis of the $\mathbf{6}^{4+}$ macrocycle. The fused polyaromatic dibenzofuran spacer makes the cavity and, hence, the distance between the two paraquat subunits much larger than in cyclophanes possessing smaller connector units such as p-phenylene ($K_a = 5600\,\mathrm{M}^{-1}$).[30d] As a consequence of the increased width of the cavity, the BHEEN molecule fits less than ideally into the macrocyclic void of the cyclophane. In order to maximize stabilization through $\pi-\pi$ stacking interactions, the cyclophane must distort itself, bending the viologen subunits inwards toward the center of the cavity. Solutions containing equimolar amounts of $\mathrm{FeCp_2}$ and the tetracationic cyclophane $\mathbf{10}\cdot 4PF_6$ in MeCN are green as a result of charge-transfer interactions between the π-electron-rich cyclopentadienyl rings of the metallocene and the π-electron-deficient viologen units of the macrocycle. The association constant observed for the $[\mathbf{10}\cdot\mathrm{FeCp_2}]^{4+}$ complex is small and is characteristic of these systems.[14, 15] Neither the $[\mathbf{6}\cdot\mathrm{BHEEN}]^{4+}$ nor the $[\mathbf{10}\cdot\mathrm{FeCp_2}]^{4+}$ complex could be observed in the "gas phase"—the LSI mass spectra of 1:1 solutions containing the constituents of each complex displayed only peaks for the tetracationic cyclophanes and its associated template. Nonetheless, the formation of both complexes in solution was ascertained by ^{1}H NMR spectroscopy (vide infra). The presence of the dicationic viologen unit in the covalent framework of the $[\mathbf{4}-\mathrm{H}]^{3+}$ system ensures that a pseudorotaxane,[39] in which one of the sidearms of the trication is inserted through the cavity of the macrocyclic polyether, is formed with BPP34C10. Solutions of BPP34C10 and $\mathbf{4}-\mathrm{H}\cdot 3PF_6$ assume a deep red color as a result of charge-transfer interactions, qualitatively indicating a large binding constant for the $[\mathbf{4}-\mathrm{H}\cdot\mathrm{BPP34C10}]^{3+}$ adduct. Indeed, the calculated value of K_a (Table 1) is somewhat higher than would be expected from comparison with similar systems,[40] perhaps indicating some interaction of the macrocyclic polyether with *both* sidearms of the trication. Moreover, the observed association constant contrasts with that of systems bearing only 4,4′-pyridylpyridinium units that are not bound by BPP34C10.[25] The presence of the pseudorotaxane complex in the "gas phase" was also corroborated by the manifestation of peaks at m/z 1333 and 1187 in the LSI mass spectrum, individually corresponding to the $[\mathbf{4}-\mathrm{H}\cdot\mathrm{BPP34C10}][PF_6]_2$ and $[\mathbf{4}\cdot\mathrm{BPP34C10}][PF_6]$ species.

^{1}H NMR Spectroscopy: The formation of the inclusion complexes $[\mathbf{6}\cdot\mathrm{BHEEN}]^{4+}$, $[\mathbf{10}\cdot\mathrm{FeCp_2}]^{4+}$, and $[\mathbf{4}-\mathrm{H}\cdot\mathrm{BPP34C10}]^{3+}$ is indicated by the ^{1}H NMR chemical shift data in Table 2. The ^{1}H NMR spectra of all of these 1:1 complexes exhibit time-averaged sets of signals, indicating that the rate of complexation and decomplexation is rapid on the ^{1}H NMR timescale.[41] The small chemical shift changes detected for both components of the $[\mathbf{6}\cdot\mathrm{BHEEN}]^{4+}$ complex may be compared with the low association constant observed for this 1:1 complex, thereby reflecting the fact that the complementary π-electron-rich and π-electron-deficient sites are too far apart in the complex to achieve optimal $\pi-\pi$ stacking. Similarly, we noticed small chemical shift changes (on account of the second-sphere coordination[42] established by $\pi-\pi$ stacking interactions between the π-electron-

Table 2. ^{1}H NMR chemical shift data (δ values) for compounds and complexes in CD_3CN or $(CD_3)_2CO$ at 20 °C.

	Polycationic Component				Neutral Component		
	α-CH	β-CH	CH_2N^+	Dbf CH [e]	ArH	OCH_2	CpH
BHEEN [a]	–	–	–	–	6.95, 7.39, 7.81	3.62, 3.92, 4.27	–
6·$4PF_6$ [a]	8.89	8.25	5.92	7.76, 7.83, 8.00	–	–	–
[**6**·BHEEN][PF_6]$_4$ [a,d,g]	8.88	8.19	5.91	7.75, 7.84, 8.00	6.91, 7.31, 7.71	3.63, 3.91, 4.25	–
BPP34C10 [b]	–	–	–	–	6.78	3.63, 3.79, 3.98	–
5·$4PF_6$ [b]	9.26	8.32	6.30	7.88, 7.97, 8.22	6.03	3.61–3.83	–
$FeCp_2$ [a]	–	–	–	–	–	–	4.15
10·PF_6 [a]	8.93	8.24	5.94	7.43, 7.68, 8.15	–	–	–
[**10**·$FeCp_2$][PF_6]$_4$ [a,d,g]	8.91	8.13	5.92	7.46, 7.70, 8.19	–	–	4.02
9·$4PF_6$ [b,c]	9.20	8.17	6.13	7.84, 8.13, 8.32	3.97 [f], 6.19	3.41, 3.68, 3.76–4.11	–
4–H·$3PF_6$ [b]	9.11, 9.44	8.35, 8.71	6.30	7.81, 7.92, 8.42	–	–	–
[**4**–H·BPP34C10][PF_6]$_3$ [b,d,h]	9.00, 9.30	8.05, 8.42	6.30	7.85, 7.96, 8.44	6.45	3.75, 3.78	–
[**4**–H·BPP34C10][PF_6]$_3$ [b,d,i]	8.98, 9.26	7.99, 8.38	6.30	7.85, 7.96, 8.44	6.35	3.74, 3.81	–

[a] Spectra obtained in CD_3CN. [b] Spectra recorded in $(CD_3)_2CO$. [c] Spectrum recorded at 253 K. [d] Spectra of an equimolar solution of both components. [e] Protons situated on the dibenzofuran moiety. [f] The identity of this resonance was ascertained from a saturation transfer experiment. [g] The concentration of both components was 5.5×10^{-3} M. [h] The concentration of both constituents was 6.0×10^{-3} M. [i] The concentration of both components was 2.7×10^{-2} M.

rich cyclopentadienyl rings of the metallocene and the π-electron-deficient viologen units of the cyclophane) for the resonances of the components of the [**10**·$FeCp_2$]$^{4+}$ inclusion complex. On the other hand, both the bipyridinium units of the [**4**–H]$^{3+}$ trication and the hydroquinone units of the macrocyclic polyether BPP34C10 are shifted far upfield in 1:1 solutions of both of these components, indicating a strong degree of intercomponent association between each of the constituents of this complex as a result of π–π stacking and other interactions. Moreover, these shifts become more pronounced at higher concentration (Table 2), perhaps indicating the formation of a hydrogen-bonded pseudopolyrotaxane with extended donor–acceptor π–π stacking interactions, as observed in the solid state (vide infra).

The tricationic salt **4**–H·$3PF_6$ exhibits (Table 2) a ^{1}H NMR spectrum wherein both of the benzyl rings of the dibenzofuran system and both of the viologen rings appear to be equivalent, that is, ancillary protons on distinct [**4**–H]$^{3+}$ units undergo rapid exchange between the nitrogen atoms of the heterocyclic extremities of the trication. These peaks were only slightly broadened when the solution was cooled down to 183 K: that is, we could not obtain quantitative information concerning the exchange process. Nevertheless, when the α-protons located adjacent to the terminal nitrogen atoms were irradiated at −10 °C we detected an NOE for the broad peak (encountered because of water and exchangeable protons) located at ca. $\delta = 5.6$, thus proving the existence of the protonated nitrogen atom. When this $(CD_3)_2CO$ solution of **4**–H·$3PF_6$ (2.7×10^{-2} M) was diluted (6.0×10^{-3} M) this resonance was shifted to higher field ($\Delta\delta = -1.1$), indicating decreased amounts of [N^+–H···N] hydrogen bonding at lower concentration. This contrasts with the other resonances of the [**4**–H]$^{3+}$ trication, the chemical shifts of which were not concentration-dependent.

^{1}H NMR chemical shift data for both the catenanes **5**·$4PF_6$ and **9**·$4PF_6$ are also reported in Table 2. The kinetic and thermodynamic parameters[43] for the circumrotation of the BPP34C10 component(s) through the cavities of the tetracationic cyclophane (process 1)[44] of the catenanes were evaluated (Table 3). In the [2]catenane **5**·$4PF_6$, it is not possible to distinguish between the "inside" and "alongside" environments of the hydroquinone ring protons, even at a temperature as low as 210 K. An estimated value of the activation energy barrier for process 1 was obtained by assuming the half-height linewidth ($\omega_{1/2}$) to be 2 Hz in the absence of exchange. The value obtained (12.6 kcal mol^{-1}) shows a decrease of almost 3 kcal mol^{-1} when compared[25] with the corresponding process for the [2]catenane **11**·$4PF_6$, in which the bipyridinium units of the tetracationic cyclophane are linked by *p*-xylyl spacers. This presumably reflects the presence of a larger cavity in the tetracationic cyclophane **5**·$4PF_6$ and, hence, the substantially reduced stabilization provided by the π-acceptor/π-donor/π-acceptor recognition motif. Table 3 also gives the activation energy barrier associated with process 2,[44] involving the circumrotation of the tetracationic cyclophane through the cavity of the BPP34C10 macrocycle, for the [2]catenane **5**·$4PF_6$. Once again, the calculated value for this exchange process is ca. 1 kcal mol^{-1} lower than that for the same process observed in the [2]catenane **11**·$4PF_6$,[25] similarly highlighting the weaker aryl–aryl stacking interactions in **5**·$4PF_6$, when compared with its congeners possessing smaller spacer units between the bipyridinium moieties. In the ^{1}H NMR spectrum of the [3]catenane **9**·$4PF_6$ (recorded in $(CD_3)_2CO$ at ambient temperature), the signals for the alongside hydroquinone ring protons are not evident; they are too broad to be observed and are assimilated into the spectrum baseline. This feature shows that the circumrotation of the BPP34C10 macrocycles through the central void of the tetracationic cyclophane in **9**·$4PF_6$ (i.e., process 1[44]) is much slower than in the related [3]catenane **12**·$4PF_6$,[35] in which the 3,7-dimethyldibenzofuran spacer

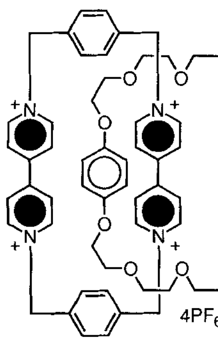

11·$4PF_6$

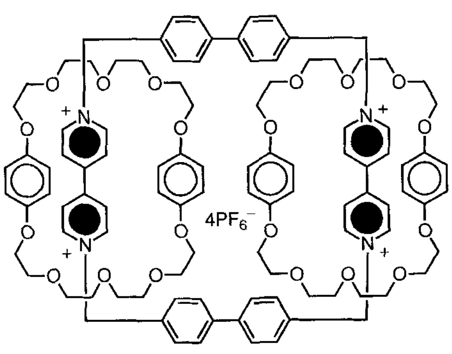

12·4PF6

units are replaced by *p,p*′-bitolyl units. Accordingly, we have estimated (Table 3) that the free energy of activation for the circumrotation of the macrocyclic polyether rings through the cavity of the tetracationic cyclophane is some 2.2 kcal mol^{-1} greater for **9**·4PF$_6$ than for the comparable circumrotation in the congener **12**·4PF$_6$. This probably relates to the reduced width of the cyclophane cavity in the former (verified by X-ray crystallography, vide infra) which makes the circumrotation of the crown ether rings through the cyclophane central void more difficult.

Table 3. Kinetic and thermodynamic parameters [a] relating to the proposed processes 1 and 2 obtained from the temperature-dependent 400 MHz ^{1}H NMR spectra recorded for the [2]catenane **5**·4PF$_6$ and the [3]catenane **9**·4PF$_6$ in $(CD_3)_2CO$.

Catenane	Probe protons	$\Delta\nu$ [a] (Hz) ($\Delta\nu$) [b]	k_c [a] (s^{-1}) (k_{ex}) [b]	T_c [a] (K) (T_{ex}) [b]	$\Delta G_c^{\ddagger}$ [a] (kcal mol^{-1}) ($\Delta G_{ex}^{\ddagger}$) [b]	Process
	OC_6H_4O	(26)	(82)	(260)	(12.6) [c]	1
5·4PF$_6$	α-CH	187	187	237	11.4	2
	β-CH	80	178	232	10.8	2
9·4PF$_6$	OC_6H_4O	888	1970	304	12.9	1

[a] Unparenthesized data relate to the coalescence method (ref. [43a]). (b) Parenthesized data relate to the exchange method (ref. [43b]). [c] For calculation of the data, it was assumed that $\omega_{1/2}$ is 6 Hz in a situation of no exchange (see text for details).

X-Ray Crystallography: The presence in the X-ray crystal structure (Figure 2) of three PF$_6^-$ anions, coupled with the unambiguous location of only a single hydrogen atom attached to one of the 4-pyridyl rings, confirmed the 4,4′-pyridylpyridinium–dibenzofuran–bipyridinium constitution of the [**4**–H]$^{3+}$ trication. The presence of complementary hydrogen bond donor (bipyridinium) and acceptor (4,4′-pyridylpyridinium) units within the covalent framework of the trication establishes its ability to behave as a plerotopic tecton. The dibenzofuran moiety has a planar geometry, but both the 4,4′-pyridylpyridinium and bipyridinium units exhibit twists between their heterocyclic rings. Whereas in the monocationic unit this twist angle (12°) is relatively small, in the dicationic unit it is large (56°). On account of the complementary hydrogen bonding sites being directed in a horseshoe-like fashion by the fused polyaromatic dibenzofuran nucleus, pairs of C_i-related tectons are linked by the [N$^+$–H···N] supramolecular synthon[45] (N···N, H···N distances 2.76, 1.87 Å, [N$^+$–H···N] angle 168°) to form (Figure 3) a noncovalently-linked "macrocycle",[16a, 46] that is, a two-component supermolecule,[47] possessing a cavity with an approximate length and breadth of 20.8 and 7.7 Å, respectively. The included Me$_2$CO and Et$_2$O molecules are located within this cavity. Inspection of the packing of these supramolecular macrocycles reveals (Figure 4) both the dibenzofuran[48] and the 4,4′-pyridylpyridinium subunits to be involved in extended π–π stacking interactions to form a two-dimensional mosaic-like sheet. The mean interplanar stacking separation for the 4,4′-pyridylpyridinium units is 3.7 Å, while that for the dibenzofuran moieties is 3.4 Å. Adjacent sheets are appreciably offset with respect to each other but there are still channels within which the anions and solvent molecules are located.

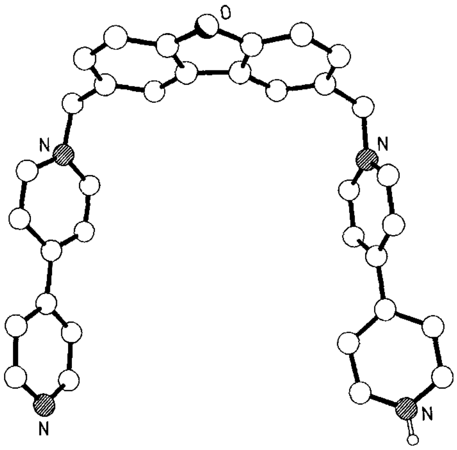

Figure 2. The covalent framework of the [4–H]$^{3+}$ trication.

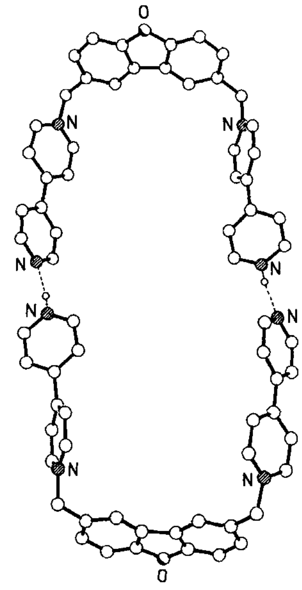

Figure 3. Ball-and-stick portrayal of the supramolecular macrocycle produced by the noncovalent dimerization of the [4–H]$^{3+}$ trication.

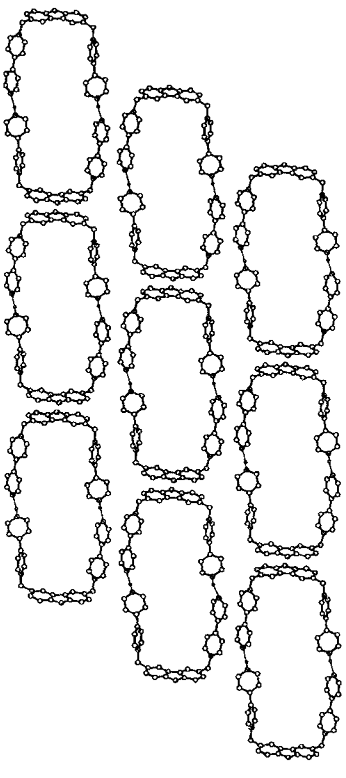

Figure 4. Ball-and-stick view of the two-dimensional mosaic-like sheet produced by the noncovalent polymerization of the [(4–H)$^{3+}$]$_2$ supramolecular macrocycle.

The solid-state structure[49] (Figure 5) of the 1:1 complex formed between [**4**–H]$^{3+}$ and BPP34C10 shows the horseshoe-shaped trication to have one of its sidearms inserted through

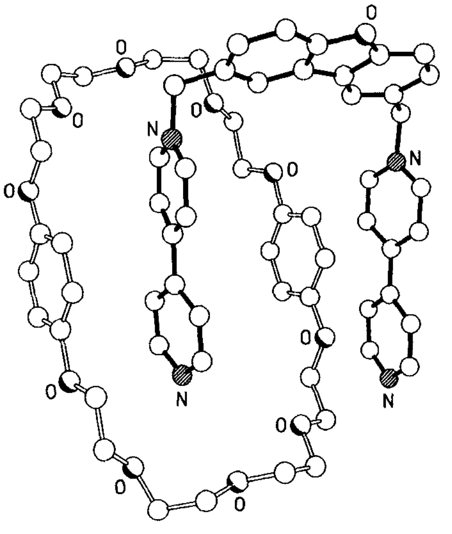

Figure 5. Ball-and-stick representation of the [**4**-H·BPP34C10]$^{3+}$ pseudorotaxane.

the center of the crown ether cavity; this arm is sandwiched between the two hydroquinone rings, while the other is positioned alongside one of the hydroquinone rings. The mean interplanar separations between the inside and alongside hydroquinone rings and the inside arm 4.1 and 3.7 Å, respectively, while the separation between the inside hydroquinone ring and the alongside arm is 3.8 Å. The twisting angles between the heterocyclic rings within each cationic component are 15° (inside) and 9° (alongside). It was not possible from the X-ray data to establish which of the two terminal nitrogen atoms is protonated. As with the free trication, the tectons are linked by $[\mathrm{N}^+{-}\mathrm{H}\cdots\mathrm{N}]$ hydrogen bonds (2.67, 2.76 Å). However, in contrast to the supramolecular macrocycle formation observed with free [**4**-H]$^{3+}$, the self-complementary tectons here are linked end-to-end to form a hydrogen-bonded pseudopolyrotaxane[50] superstructure, that is, a supramolecular array,[51] in which the pattern of π-donor/π-acceptor stacking extends to include both the alongside hydroquinone rings and the alongside sidearm (Figure 6). The mean interplanar stacking separation between these two latter components is 3.8 Å. Unlike in free [**4**-H]$^{3+}$, here there is no stacking of adjacent dibenzofuran ring systems.

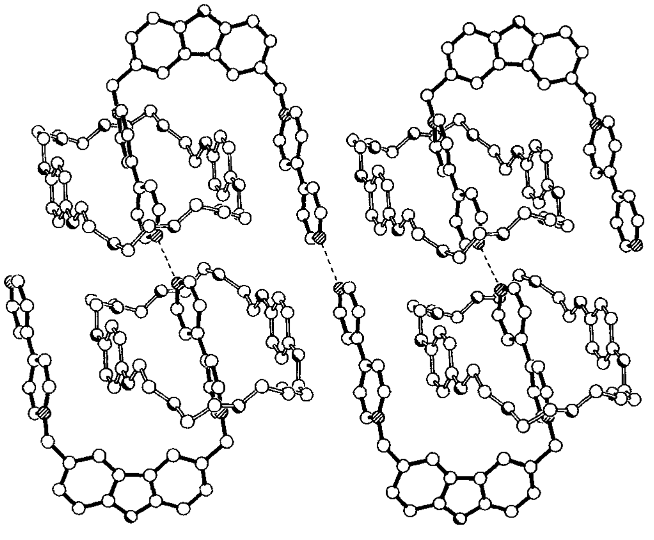

Figure 6. Ball-and-stick view of part of the hydrogen-bonded pseudopolyrotaxane superstructure produced by the noncovalent polymerization of the [**4**-H·BPP34C10]$^{3+}$ pseudorotaxane.

In terms of the demeanor of the hydrogen-bonded superstructure produced by the [**4**-H]$^{3+}$ trication, the difference in the crystal structures between the uncomplexed tecton and its BPP34C10 cocrystal amounts to a notable superstructural change from a dimeric supermolecule to a polymolecular supramolecular array (Scheme 4).[52] This system may also represent a prototypical solid-state supramolecular device:[1b, 7, 8f] by opening the noncovalently-linked supramolecular macro cycle, the macrocyclic polyether BPP34C10 effects mechanical switching from the closed supramolecular macrocycle to the open, pseudopolyrotaxane supramolecular array.

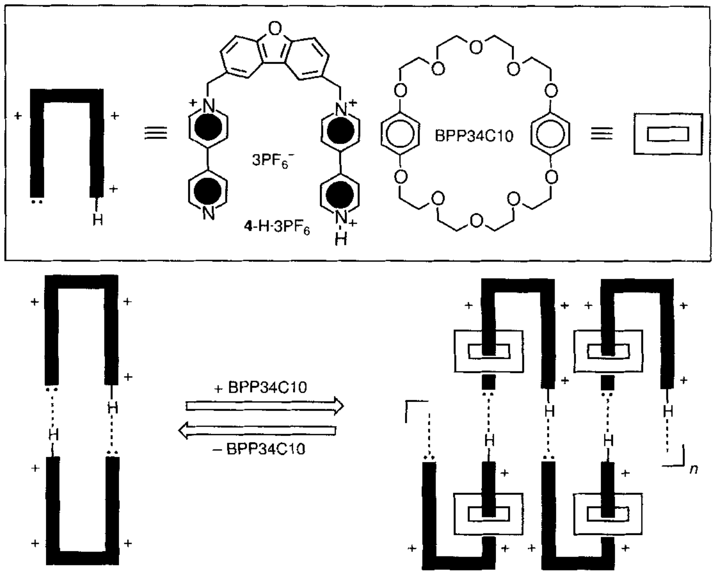

Scheme 4. Schematic presentation of the BPP34C10-mediated interconversion between the dimeric [(**4**-H)$^{3+}$]$_2$ supramolecular macrocycle and the pseudopolyrotaxane supramolecular array, produced by noncovalent polymerization of the [**4**-H·BPP34C10]$^{3+}$ pseudorotaxane, in the solid state.

The X-ray structural analysis (Figure 7) of **6**·4PF$_6$ shows it to possess an open cyclophane-like structure with approximate C_i symmetry and overall dimensions of ca. 8.5 × 11.8 Å. The two dibenzofuran moieties are consequently oriented in an *anti* geometry with respect to one another and are seen to be tilted by ca. 63° and 66° with respect to the mean plane of the macrocycle (as defined by the four methylene carbon atoms). The two bipyri-

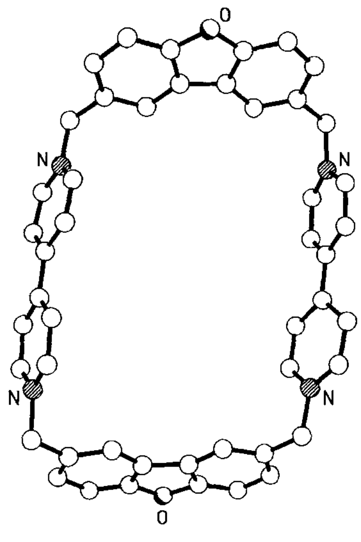

Figure 7. Ball-and-stick representation of the covalent framework of the **6**$^{4+}$ cyclophane.

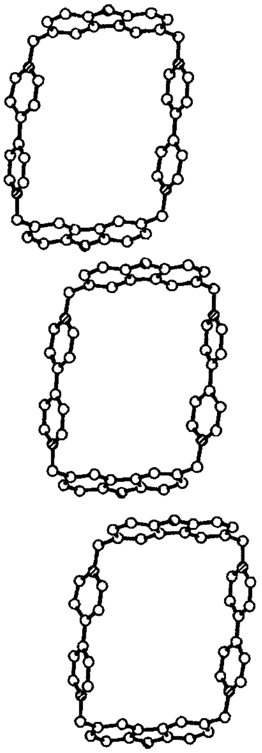

Figure 8. Ball-and-stick representation of the self-assembled tape produced by the noncovalent polymerization of the $\mathbf{6}^{4+}$ cyclophane.

dinium units exhibit twisting (2°, 15°) and bowing (11°, 14°) distortions, their overall mean planes both being tilted in the same direction with respect to the mean plane of the macrocycle, that is, a shearing deformation. This deformation is slight and does not produce any significant reduction in the free pathway through the macrocyclic center. Both dibenzofuran moieties are involved in $\pi-\pi$ stacking interactions[48] (Figure 8) with their C_i related counterparts with a mean interplanar separation of 3.4 Å in both instances, to form a self-assembled tape, produced by the solid state noncovalent polymerization of the $\mathbf{6}^{4+}$ tetracationic macrocycle. The bipyridinium units, on the other hand, are not involved in any intercation stacking interactions. Viewed down the crystallographic *c* direction (Figure 9), adjacent cyclophanes are seen to form nanotube-like channels[53] with a cross-section free pathway of ca. 5.5 Å, though with alternate macrorings rotated in plane by ca. 90° with respect to each other. There is a small tilt of 14° of the mean plane of adjacent cyclophanes within the channel. Two of the PF_6^- anions and the included solvent molecules are positioned within the extended channels: the remaining two anions are positioned over the peripheries of the channels.

The X-ray structural analysis (Figure 10) of $\mathbf{5}\cdot 4PF_6$ reveals that it possesses the expected [2]catenane topology: one of the hydroquinone rings of the BPP34C10 macrocycles is sandwiched between the pair of bipyridinium units of the tetracationic cyclophane; the other is positioned alongside. The mean interplanar separations between the inside hydroquinone ring and the inside and alongside bipyridinium units are 3.7 and 3.6 Å, respectively, and that between the alongside hydroquinone ring and the inside bipyridinium unit is 3.7 Å. In addition to the $\pi-\pi$ stacking interactions, there is a single [C–H···O] hydrogen bond between one of the α-bipyridinium hydrogen atoms on the inside unit and the central oxygen atom of one of the polyether linkages in the BPP34C10 macrocycle ([C···O], [H···O] distances 3.28, 2.37 Å, [C–H···O] angle 158°). The BPP34C10 ring has approximate C_s molecular symmetry about a plane passing through the two central oxygen atoms of the polyether linkages with both hydroquinone rings having in-plane *syn* geometries for the two OCH_2 bonds. The OC_6H_4O axis of the inside hydroquinone rings is inclined by ca. 42° to the mean plane of the tetracationic cyclophane as defined by the four corner methylene carbon atoms. The conformation of the tetracation is markedly different from that observed in its uncatenated state (vide supra). Firstly, the two dibenzofuran moieties are in a *syn* geometry (cf. *anti* in $\mathbf{6}\cdot 4PF_6$) with their planes inclined by ca. 38° and 30° to the cyclophane ring plane.[54] Secondly, and more significantly, instead of the two bipyridinium units being bowed outwards away from the ring center, here they are appreciably folded inwards so as to minimize their contact distance with the π-electron-rich inside hydroquinone ring: the inward bow angles of the inside and outside bipyridinium units are 14° and 11°, respectively.[55] Accompanying this inward bowing, there is a significant twisting about the long axis of the tetracationic cyclophane, the [N···N] axes of the two bipyridinium units being inclined by ca. 19°. In addition to bowing distortions, the bipyridinium units exhibit differing degrees of twist about the C–C bond linking the pyridinium rings. One of these twists (that associated with the alongside bipyridinium unit) is quite large (27°), while that for the inside unit is significantly smaller (16°). A consequence of these conformational distortions is a noticeable contraction in the smaller dimension of the cyclophane from 8.5 Å in $\mathbf{6}^{4+}$ to 7.4 Å in $\mathbf{5}^{4+}$ and a slight increase in its length from 11.8 Å in $\mathbf{6}^{4+}$ to 12.1 Å in $\mathbf{5}^{4+}$. Inspection of the packing of the catenanes reveals, as in many other [2]catenanes of this type,[5e, 25, 28] the formation of polar stacks extending throughout the crystal in the crystallographic *b* direction: the outside hydroquinone ring of one [2]catenane being positioned approximately parallel to, and overlapping with, one of the pyridinium rings of the outside bipyridinium unit of the next. The mean interplanar separations between these rings is 3.6 Å and the centroid–centroid separation is 4.0 Å. Unlike in the cyclophane

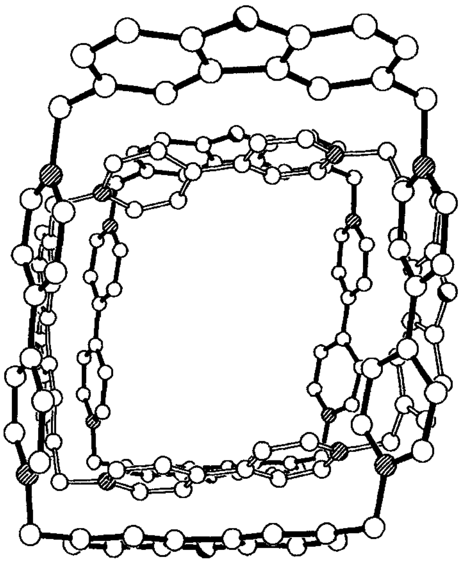

Figure 9. View of the nanotube-like channels formed by the $\mathbf{6}^{4+}$ cyclophane.

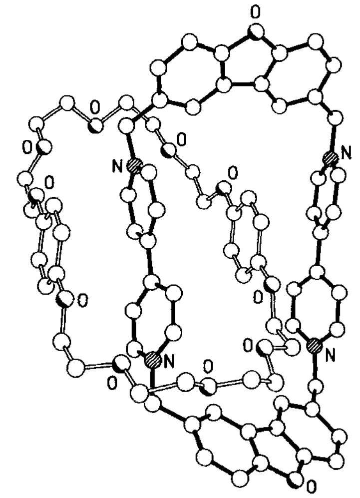

Figure 10. Ball-and-stick representation of the [2]catenane $\mathbf{5}^{4+}$.

$\mathbf{6}^{4+}$ (vide supra), there is no aryl–aryl stacking involving the dibenzofuran units.

The solid-state structure (Figure 11) of the tetracationic cyclophane $\mathbf{10}^{4+}$, isomeric with $\mathbf{6}^{4+}$, has a C_i symmetric open-box structure with a length of ca. 11.2 Å between the dibenzofuran moieties and a breadth of ca. 10.7 Å, that is, it may be considered to be an *organic molecular rectangle.* The decreased width of this organic quadrilateral, compared with that of its *p,p'*-bitolyl spaced congener $\mathbf{2}^{4+}$, may be ascribed to the influence of the dibenzofuran units: the effect of the central furan ring is to pull the *p,p'*-carbon atoms of *p,p'*-bitoluene toward itself, therefore decreasing the overall length of the spacer unit. The *anti*-disposed dibenzofuran subunits are inclined by 74° to the cyclophane ring plane. The bipyridinium units have twisting and bowing distortions of 38° and 20°, respectively. Like its 2,8-disubstituted congener $\mathbf{6}^{4+}$ (vide supra), the tetracationic macrocycles pack to form π–π stacked chains with the dibenzofuran subunits[48] in one cyclophane overlying those of the next with a mean interplanar separation of 3.3 Å. There are no π–π interactions involving the bipyridinium units, nor are any dominant channels formed in the structure.

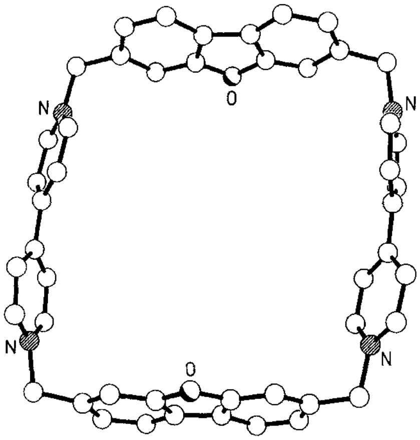

Figure 11. The covalent framework of the tetracationic cyclophane $\mathbf{10}^{4+}$.

The solid-state structure (Figure 12) of $\mathbf{9}^{4+}$ reveals it to be the anticipated [3]catenane, in which two BPP34C10 rings encircle opposite bipyridinium units of the macrocyclic tetracation component. The [3]catenane has C_i crystallographic symmetry and the separations between the planes of the inside hydroquinone rings, and between the inside bipyridinium units and the inside and outside hydroquinone rings are all 3.4 Å (the centroid–centroid separation between the two inside hydroquinone rings is 4.0 Å). The centroid–centroid separations between the edge-to-face oriented hydroquinone rings and the proximal benzenoid rings of the dibenzofuran systems are both 5.6 Å, that is, distances too large to represent any significant [C–H $\cdots\pi$] interactions. Similarly, there is a noticeable absence of any [C–H $\cdots$ O] hydrogen bonding. Despite the absence of these secondary stabilizing interactions normally present in [2]- and [3]catenanes of this type,[5e, 35] the OC_6H_4O axes of the inside hydroquinone rings are still inclined by ca. 43° to the mean plane of the cyclophane, tilt angles being very similar to those observed in related [2]- and [3]catenanes.[35] It is noteworthy that both the inside and outside hydroquinone rings have *anti* geometries associated with the OCH_2 bonds. The tetracationic cyclophane has an overall geometry very similar to that observed in its uncatenated form, the dibenzofuran subunits adopting an *anti* geometry with respect to each other, with their mean planes inclined by ca. 69° to the tetracationic cyclophane mean plane. The length and breadth show only small changes with the length increasing from 11.2 Å in $\mathbf{10}^{4+}$ to 11.7 Å in $\mathbf{9}^{4+}$ and the breadth decreasing from 10.7 to 10.5 Å, permitting near optimal π–π stacking geometry with the interlocked BPP34C10 rings. The only significant change in the conformation is a marked reduction in the twist angle between the two pyridinium rings to only 2° (cf. 38° in $\mathbf{10}^{4+}$). The bowing of the bipyridinium units is only slightly reduced (16°, cf. 20° in $\mathbf{10}^{4+}$). The [3]catenanes pack to form a two-dimensional mosaic: in one direction the dibenzofuran ring systems of lattice-translated interlocked species are involved in π–π stacking interactions[48] (interplanar separation 3.49 Å), while in the other, the outside hydroquinone rings, again of lattice-translated [3]catenanes, extend the pattern of π–π interactions that is present within the catenane itself (Figure 13):[35] the mean interplanar separation between the outside hydroquinone rings is 3.51 Å, with an associated centroid–centroid separation of 4.19 Å.

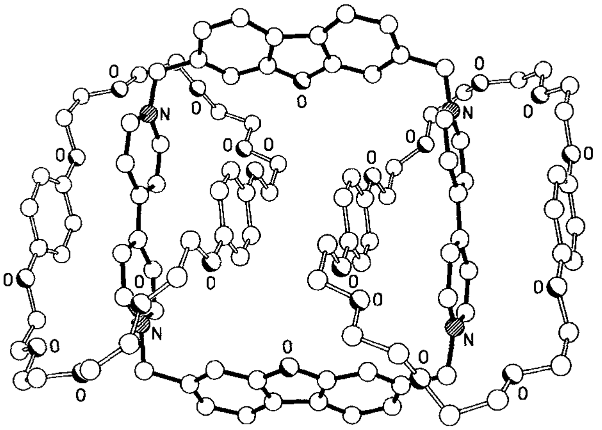

Figure 12. Ball-and-stick representation depicting the [3]catenane $\mathbf{9}^{4+}$.

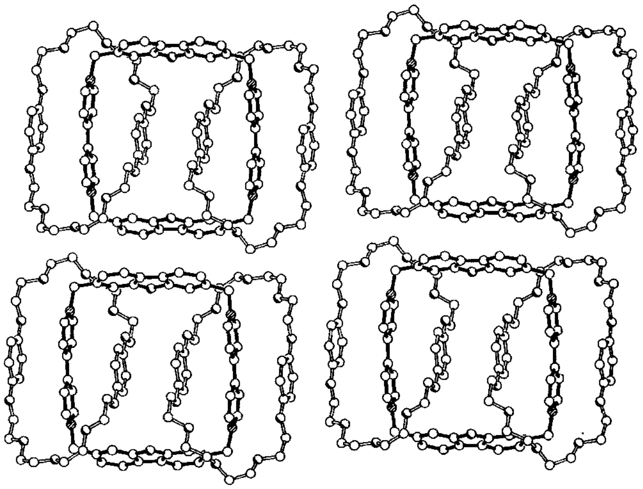

Figure 13. Ball-and-stick view of the two-dimensional mosaic formed by the supramolecular polymerization of the [3]catenane $\mathbf{9}^{4+}$.

Molecular Modeling: Molecular modeling was employed so that we could anticipate the interaction geometries for the [**6**·BHEEN]$^{4+}$ and the [**10**·FeCp$_2$]$^{4+}$ template–tetracationic cyclophane inclusion complexes. Incorporation of the template BHEEN into the cavities of both conformational isomers of the tetracationic cyclophane **6**$^{4+}$, that is, the *syn* or *anti* conformers, followed by molecular dynamics at 300 K and minimization of the samples obtained from the dynamics simulation, provided an ensemble of conformations representing the two low-energy ground state structures. The modeling study for the *anti* conformer predicts that the guest species is inserted through the center of the internal void of the tetracationic cyclophane (Figure 14) with the π-electron-deficient bipyridinium subunits located at a mean interplanar separation of approximately 3.9 Å from the center of the 1,5-dioxynaphthalene unit. Interestingly we noticed that (as in the solid state structure of the [2]catenane **5**$^{4+}$ above), there is a concave distortion of the macrocyclic periphery of the cyclophane: the angles subtended by the CH$_2$–N$^+$ bonds of the bipyridinium units are in the range 2–3°. This small "hourglass-like" distortion is presumably a consequence of the cyclophane attempting to minimize its contact distance with the included π-electron-rich guest. Additionally, it is predicted that strong, stabilizing [C–H···O] hydrogen bonding interactions exist between the terminal oxygen atoms of the hydroxyl groups of the BHEEN guest and the β-bipyridinium hydrogen atoms (H···O distance 2.7 Å). Similar observations were made for the *syn* conformational isomer, but with the notable exception that the deformation of the bipyridinium units was even more pronounced: the mean interplanar distance between the bipyridinium residues and the centroid of the naphthalene guest species is reduced to 3.8 Å. Similarly, as in the case of the *anti* conformer, there exist [C–H···O] interactions between the terminal oxygen atoms of the polyether chains and the α-bipyridinium hydrogen atoms (H···O distance 2.7–3.5 Å).

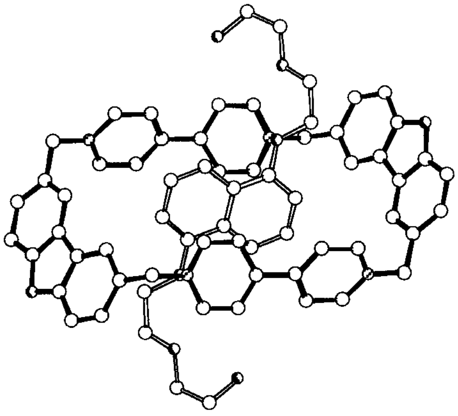

Figure 14. Computer-generated structure of the inclusion complex formed between the tetracationic cyclophane **6**$^{4+}$ and BHEEN.

Molecular mechanics calculations (with the Sybyl forcefield) on the 1:1 complex formed between the tetracationic cyclophane **10**$^{4+}$ and FeCp$_2$ reveal a complex in which the metallocene is ideally located in the center of the macrocyclic cavity. The cyclopentadienyl rings are sandwiched between the faces of the bipyridinium units (Figure 15) with a distance of ca. 3.3 Å from the center of the bond joining the two pyridinium units of the viologen system to the centroid of the cyclopentadienyl ring. The cyclophane cavity is slightly enlarged on binding in both the *syn* and *anti* conformers: the dimensions of the edges of the molecular rectangle increase from about 8.1 × 10.0 Å to about 9.9 × 10.2 Å for both the *syn* and the *anti* geometries. Single-point semiempirical calculations at the PM3tm level suggest that it is the *anti* isomer that possesses the more favorable intermolecular interactions, with the heat of formation of the complex being slightly lower in energy than that for the corresponding *syn* isomer. In addition, qualitative examination of the calculated heats of formation for the free cyclophane **10**$^{4+}$, FeCp$_2$, and the [**10**·FeCp$_2$]$^{4+}$ complex indicates a high degree of stabilizing interactions, since the complexes have a heat of formation 36 kcal mol^{-1} lower than the sum of the heats of formation of the separate constituents.

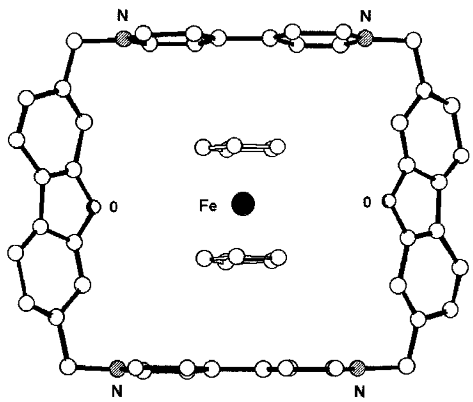

Figure 15. Computer-generated structure for the inclusion complex formed between the tetracationic cyclophane **10**$^{4+}$ and FeCp$_2$.

Conclusions

The template-directed synthesis of two organic molecular rectangles incorporating dibenzofuran units, **6**$^{4+}$ and **10**$^{4+}$, has been accomplished. We have employed a synthetic strategy in which catenanes were initially prepared in order to identify appropriate templates for the synthesis of the organic rectangles in reasonable yield.[15] These rectangles have also proved to be useful building blocks for supramolecular, noncovalent synthesis in the solid state, where they form supramolecular polymers[6] (specifically self-assembled[8] tapes consisting of tetracationic macrocycles linked by the crossed aryl–aryl stacking motif of the dibenzofuran subunits).[48] Furthermore, the cyclophane **6**$^{4+}$ forms nanotubular channels in the solid state. We believe that the anticipated solid-state π-donor/π-acceptor stacks[14] (analogous to those observed for the cyclophane **1**$^{4+}$) are not produced because of the predisposition of the dibenzofuran subunits to form the crossed π–π stacks that we have seen repeatedly in our crystal structures. This motif is even prevalent in the crystal structure of the [3]catenane **9**$^{4+}$, in which a two-dimensional mosaic is produced: the crossed aryl–aryl stacking of the dibenzofuran units proceeds in one direction, while a DAD-DAD sequence of π-donors (D) and π-acceptors (A) extends throughout the crystal in the other direction. This π–π stacking motif displayed by the dibenzofuran subunits has powerful implications for the rational design of organic solids, that is, crystal engineering,[5] and in the preparation of new supramolecular materials.[6] Moreover, we have made the serendipitous discovery of the plerotopic tecton $[\mathbf{4}-\mathrm{H}]^{3+}$, which possesses complementary hydrogen bond donor and acceptor sites. The 2,8-disubstituted dibenzofuran unit in this trication orients the complementary hydrogen bonding sites in a horseshoe-like fashion, permitting tecton dimerization in the solid state to form a supramolecular macrocycle. Conversely, cocrystallization of the tecton with BPP34C10 induces opening of the dimeric supermolecule to provide a pseudopolyrotaxane[50] supramolecular array that combines both π–π stacking and hydrogen bonding interactions. In terms of the hydrogen bonding demeanor displayed by the $\mathbf{4}-\mathrm{H}^{3+}$ tecton, the superstructural changes exhibited in the system presented here correspond to the opening of the closed $[(\mathbf{4}-\mathrm{H})^{3+}]_2$ noncovalently-linked macrocycle to form a $[(\mathbf{4}-\mathrm{H})^{3+}]_n$ noncovalent polymer (Scheme 4), perhaps implying that the system could perform as a prototypical supramolecular device.[1b, 7, 8f]

Experimental Section

Materials and Methods: Anhydrous MeCN was distilled from CaH_2 under N_2. Anhydrous DMF and CCl_4 were obtained from Aldrich in Sure/Seal® containers and stored under N_2. Bz_2O_2 was vacuum-dried for 24 h before use. Similarly, NH_4PF_6 was vacuum-dried prior to dissolution in H_2O for anion exchange procedures, except for the preparation of $\mathbf{4}-\mathrm{H}\cdot 3PF_6$. NH_4PF_6 was considered to be suitable for use when it was odorless. Flash chromatography was carried out under the usual conditions,[56] except that we employed a flow rate of 3.8 cm min^{-1}. Conventional percolation column chromatography was performed on silica gel 60 (Merck 9385, 230–400 mesh). Melting points were determined with an Electrothermal 9200 melting point apparatus and are uncorrected. Proton and ^{13}C NMR spectra were recorded on a Bruker AC300 spectrometer (at 300 and 75 MHz, respectively) or on a Bruker AMX 400 (at 400 and 100 MHz, respectively) with the deuterated solvent as the lock and the residual solvent as internal reference. Liquid secondary-ion mass spectra (LSIMS) were obtained with a VG Zabspec mass spectrometer equipped with a cesium ion source and using a *m*-nitrobenzyl alcohol matrix. Electron-impact mass spectra (EIMS) were obtained from a VG Prospec mass spectrometer. Microanalyses were performed by the University of North London Microanalytical Services. The crystal growing methods used were as described by Jones.[57]

2,8-Bis(chloromethyl)dibenzofuran (3): The procedure used was similar to one reported in the Russian literature.[23] A suspension of paraformaldehyde (45.0 g, 1.5 mol) in AcOH (250 mL) and H_3PO_4 (29 mL, 85 wt% in H_2O) was heated to 100 °C with vigorous stirring until a clear, homogeneous solution was obtained. The solution was cooled to ambient temperature and then 12 N HCl (148 mL) was added to the stirred solution. Dry HCl gas was bubbled through the cloudy solution with stirring for 0.5 h until the solution became clear again. At this point, dibenzofuran (16.8 g, 0.1 mol) was added all at once. Gas addition was continued and, after 2 h, the temperature of the reaction mixture was raised to 50 °C. The temperature was increased to 80 °C after a further 2 h, and then ultimately increased to 90 °C 2 h later. Finally, 7.5 h after the addition of the dibenzofuran, the reaction mixture was poured into H_2O (2 L). The resulting precipitate was collected and washed thoroughly with H_2O (4 L) and air-dried. Several recrystallizations of the residue from $i\mathrm{Pr}_2O$ provided 16.3 g (62%) of **3** as a white solid. M.p. 125 °C (ref. [23] m.p. 128–130 °C); ^1H NMR (300 MHz, $CDCl_3$, 20 °C): $\delta = 4.75$ (s, 4H), 7.47 (dd, $J = 8, 1$ Hz, 2H), 7.54 (d, $J = 8$ Hz, 2H), 7.96 (d, $J = 1$ Hz, 2H); ^{13}C NMR (75 MHz, $CDCl_3$, 20 °C): $\delta = 46.5$, 112.1, 121.1, 124.2, 128.3, 132.4, 156.5; EIMS: $m/z = 264$ $[M]^+$; $C_{14}H_{10}Cl_2O$ (265.1): calcd C 63.42, H 3.80; found C 63.49, H 3.87.

1,1′-[2,8-Dibenzofuranbis(methylene)]bis-4,4′-pyridylpyridinium bis(hexafluorophosphate) ($\mathbf{4}\cdot 2PF_6$): A solution of 2,8-bis(chloromethyl)dibenzofuran **3** (0.26 g, 1.0 mmol) in anhydrous MeCN (15 mL) was added dropwise with stirring to a refluxing solution of 4,4′-bipyridine (1.09 g, 7.0 mmol) in anhydrous MeCN (10 mL) for 3 h under N_2. The solution was heated under reflux for a further 45 h and then treated with Et_2O (60 mL) on cooling. The remaining greenish solid was collected and washed with Et_2O (50 mL), before being dissolved in a small amount of a hot 60% MeOH/20% H_2O/20% saturated aqueous NH_4Cl solution and subjected to flash chromatography with the same solvent. The fractions containing the product were combined and the solvents evaporated. The residue was dissolved in warm H_2O. The title compound $\mathbf{4}\cdot 2PF_6$ precipitated out of solution upon addition of a concentrated aqueous solution of NH_4PF_6. The remaining white solid was collected, washed with H_2O, and dried (0.34 g, 43%). M.p. 156 °C with decomp.; ^1H NMR (300 MHz, $(CD_3)_2CO$, 20 °C): $\delta = 6.27$ (s, 4H), 7.81 (d, $J = 9$ Hz, 2H), 7.91 (dd, $J = 9, 2$ Hz, 2H), 7.95 (d, $J = 6$ Hz, 4H), 8.45 (d, $J = 2$ Hz, 2H), 8.64 (d, $J = 7$ Hz, 4H), 8.85 (d, $J = 6$ Hz, 4H), 9.38 (d, $J = 7$ Hz, 4H); ^{13}C NMR (75 MHz, $(CD_3)_2CO$, 20 °C): $\delta = 65.1$, 113.7, 121.2, 123.6, 125.4, 127.1, 129.6, 130.4, 142.1, 146.1, 151.9, 155.1, 157.9; LSIMS: $m/z = 651$ $[M - PF_6]^+$; $C_{34}H_{26}F_{12}N_4OP_2$ (796.5): calcd C 51.27, H 3.29, N 7.03; found C 51.07, H 3.15, N 6.97.

Plerotopic Tecton $\mathbf{4}-\mathbf{H}\cdot\mathbf{3PF_6}$: A similar procedure to the one described above was employed to prepare $\mathbf{4}\cdot 2Cl$ from **3** (0.53 g, 2.0 mmol) and 4,4′-bipyridine (2.18 g, 14.0 mmol). After evaporation of the solvents from flash chromatography, the residue was dissolved in warm H_2O and a concentrated aqueous solution of practical grade NH_4PF_6 (Aldrich, 95+ %) was added until precipitation was complete. The precipitate was collected and recrystallized from $Me_2CO/MeOH/H_2O$ to give 0.78 g (41%) of $\mathbf{4}-\mathrm{H}\cdot 3PF_6$ as white flakes. M.p. 221–225 °C; ^1H NMR (300 MHz, $(CD_3)_2CO$, 20 °C): $\delta = 5.60$ (brs, 1H), 6.30 (s, 4H), 7.81 (d, $J = 8$ Hz, 2H), 7.92 (dd, $J = 8, 2$ Hz, 2H), 8.35 (d, $J = 7$ Hz, 4H), 8.42 (d, $J = 2$ Hz, 2H), 8.71 (d, $J = 7$ Hz, 4H), 9.11 (d, $J = 7$ Hz, 4H), 9.44 (d, $J = 7$ Hz, 4H); ^{13}C NMR (75 MHz, $(CD_3)_2CO$, 20 °C): $\delta = 65.3$, 113.7, 123.7, 125.1, 125.4, 127.8, 129.6, 130.5, 146.5, 147.3, 148.2, 153.7, 158.0; LSIMS: $m/z = 651$ $[M - HPF_6 - PF_6]^+$; $C_{34}H_{27}F_{18}N_4OP_3$ (942.5): calcd C 43.33, H 2.89, N 5.94; found C 43.09, H 2.84, N 5.79. Single crystals, suitable for crystallographic analysis, were obtained by liquid diffusion of Et_2O into an $EtOH/Me_2CO$ solution of $\mathbf{4}-\mathrm{H}\cdot 3PF_6$.

{[2]-[Cyclobis(paraquat-2,8-dibenzofuran)]-[BPP34C10]-catenane} Tetrakis(hexafluorophosphate) ($\mathbf{5}\cdot 4PF_6$): A solution of BPP34C10 (108 mg, 0.20 mmol), $\mathbf{4}\cdot 2PF_6$ (79 mg, 0.10 mmol), 2,8-bis(chloromethyl)dibenzofuran **3** (34 mg, 0.13 mmol), and a catalytic amount of NaI (2 mg, 0.01 mmol) in anhydrous MeCN (5.5 mL) was stirred under N_2 at 20 °C for 19 d. The solution was concentrated in vacuo and the residue was dissolved in a small amount of a hot 70% MeOH/10% $MeNO_2$/20% 2 M aqueous NH_4Cl solution, before being subjected to percolation column chromatography with the same solvent. The fractions containing the product were combined and the solvents evaporated. The residue was dissolved in warm aqueous MeOH. The catenane $\mathbf{5}\cdot 4PF_6$ precipitated out of solution upon addition of a concentrated aqueous solution of NH_4PF_6. The remaining orange solid was collected, washed with H_2O and dried (55 mg, 30%). M.p. 261 °C with decomp.; ^1H NMR (300 MHz, $(CD_3)_2CO$, 20 °C): $\delta = 3.61$–3.83 (m, 32H), 6.03 (s, 8H), 6.30 (s, 8H), 7.88 (d, $J = 9$ Hz, 4H), 7.97 (d, $J = 9$ Hz, 4H), 8.22 (s, 4H), 8.32 (d, $J = 7$ Hz, 8H), 9.26 (d, $J = 7$ Hz, 8H); ^{13}C NMR (100 MHz, $(CD_3)_2CO$, 31 °C): $\delta = 65.2$, 68.6, 70.8, 71.1, 71.2, 113.2, 115.7, 122.0, 125.8, 126.9, 130.4, 131.2, 147.2, 148.9, 153.0, 158.0; LSIMS: $m/z = 1671$ $[M - PF_6]^+$; $C_{76}H_{76}F_{24}N_4O_{12}P_4$ (1817.3): calcd C 50.23, H 4.22, N 3.08; found C 50.07, H 3.91, N 3.11. Single crystals, suitable for X-ray crystallographic analysis, were grown by vapor diffusion of PhH into a $MeNO_2$ solution of the catenane.

Cyclobis(paraquat-2,8-dibenzofuran) Tetrakis(hexafluorophosphate) ($\mathbf{6}\cdot 4PF_6$): A solution of $\mathbf{4}\cdot 2PF_6$ (79 mg, 0.10 mmol), BHEEN (119 mg, 0.35 mmol), 2,8-bis(chloromethyl)dibenzofuran **3** (30 mg, 0.11 mmol), and NaI (7 mg, 0.05 mmol) in anhydrous MeCN (21 mL) was stirred under N_2 at 20 °C for 15 d, after which the reaction mixture was poured into Et_2O (160 mL). The resultant red precipitate was collected and washed further with Et_2O (50 mL) before being dissolved in a 70% MeOH/10% $MeNO_2$/20% 2 M aqueous NH_4Cl solution, and subjected to percolation column chromatography with the same solvent. The fractions containing the product were combined and the solvents evaporated. The residue was dissolved in warm H_2O, filtered, then treated with a concentrated aqueous solution of NH_4PF_6. The

0947-6539/97/0307-1146 $ 17.50+.50/0

precipitate generated was collected, washed with H_2O, and dried to afford **6**·4PF_6 as a white solid (63 mg, 49%). M.p. 272 °C with decomp.; ^{1}H NMR (300 MHz, CD_3CN, 20 °C): δ = 5.92 (s, 8H), 7.76 (d, J = 8 Hz, 4H), 7.83 (d, J = 8 Hz, 4H), 8.00 (s, 4H), 8.25 (d, J = 7 Hz, 8H), 8.89 (d, J = 7 Hz, 8H); ^{13}C NMR (75 MHz, CD_3CN, 20 °C): δ = 65.6, 113.4, 123.3, 125.8, 128.2, 129.1, 129.8, 131.7, 146.4, 150.8; LSIMS: m/z = 1135 $[M - PF_6]^+$; $C_{34}H_{26}F_{12}N_4OP_2$ (1280.7): calcd C 45.02, H 2.83, N 4.37; found C 44.96, H 2.71, N 4.47. Single crystals, suited for X-ray crystallographic analysis, were grown by vapor diffusion of $i$$Pr_2O$ into a solution of **6**·4PF_6 in $MeNO_2$.

3,7-Bis(bromomethyl)dibenzofuran (7): This dibromide was prepared by an adaptation of Weber and Kormany's procedure.[34] A solution containing a catalytic amount of Bz_2O_2 (12 mg) and 3,7-dimethyldibenzofuran[58] (1.76 g, 9.0 mmol) in anhydrous CCl_4 (36 mL) was heated with stirring to 70 °C (bath). NBS (3.20 g, 18.0 mmol) and more Bz_2O_2 (46 mg) were added to the solution in small portions over a period of 15 min. Thereafter, the reaction mixture was heated under reflux with stirring under slight N_2 pressure for 3 h. The reaction mixture was cooled to 20 °C, then the resulting precipitate was collected and recrystallized from CCl_4 to give 1.36 g (43%) of the title compound **7** as a white solid. M.p. 205–208 °C (ref. [34] m.p. 193–194 °C); ^{1}H NMR (300 MHz, $CDCl_3$, 20 °C): δ = 4.65 (s, 4H), 7.37 (dd, J = 8, 1 Hz, 2H), 7.59 (d, J = 1 Hz, 2H), 7.88 (d, J = 8 Hz, 2H); ^{13}C NMR (75 MHz, $CDCl_3$, 20 °C): δ = 33.7, 112.3, 121.0, 124.0, 124.1, 137.4, 156.6; EIMS: m/z = 354 $[M]^+$; $C_{14}H_{10}Br_2O$ (354.0): calcd C 47.50, H 2.85; found C 47.51, H 2.96.

1,1′-[3,7-Dibenzofuranbis(methylene)]bis-4,4′-pyridylpyridinium bis(hexafluorophosphate) (8·2PF_6): A solution of **7** (0.25 g, 0.7 mmol) in anhydrous DMF (12 mL) was added dropwise with stirring to a refluxing solution of 4,4′-bipyridine (0.77 g, 4.9 mmol) in anhydrous MeCN (5 mL) over a period of 1 h under N_2. The solution was heated under reflux for a further 20 h, before being treated with Et_2O (40 mL) upon cooling. The remaining solid was collected, washed with Et_2O (40 mL), dissolved in a small amount of a hot 60% MeOH/20% H_2O/20% saturated aqueous NH_4Cl solution, and thereupon subjected to flash chromatography with the same solvent. The fractions containing the product were combined and the solvents evaporated. The residue was dissolved in warm H_2O. The title compound **8**·2PF_6 precipitated out of solution on addition of a concentrated aqueous solution of NH_4PF_6. The remaining solid was collected and recrystallized from EtOH/Me_2CO/H_2O to give **8**·2PF_6 as a white solid (0.43 g, 86%). M.p. 169 °C with decomp.; ^{1}H NMR (300 MHz, $(CD_3)_2CO$, 20 °C): δ = 6.32 (s, 4H), 7.76 (d, J = 8 Hz, 2H), 7.96 (d, J = 6 Hz, 4H), 8.06 (s, 2H), 8.31 (d, J = 8 Hz, 2H), 8.71 (d, J = 7 Hz, 4H), 8.85 (d, J = 6 Hz, 4H), 9.46 (d, J = 7 Hz, 4H); ^{13}C NMR (75 MHz, CD_3CN, 20 °C): δ = 65.0, 114.0, 122.8, 123.5, 125.5, 125.7, 127.3, 133.9, 142.1, 146.0, 152.1, 155.7, 157.7; LSIMS: m/z = 651 $[M - PF_6]^+$; $C_{34}H_{26}F_{12}N_4OP_2$ (796.5): calcd C 51.27, H 3.29, N 7.03; found C 51.47, H 3.33, N 6.36.

{[3]-[BPP34C10]-[Cyclobis(paraquat-3,7-dibenzofuran)]-[BPP34C10]-catenane} tetrakis(hexafluorophosphate) (9·4PF_6): A solution of BPP34C10 (109 mg, 0.20 mmol), **8**·2PF_6 (79 mg, 0.10 mmol), and 3,7-bis(bromomethyl)dibenzofuran **7** (45 mg, 0.13 mmol) in anhydrous 60% MeCN/40% DMF (5.5 mL) was stirred under N_2 at 20 °C for 10 d. The reaction mixture was worked up, as described for the [2]catenane **5**·4PF_6, to give the [3]catenane **9**·4PF_6 as a magenta-colored solid (42 mg, 18%). M.p. 273 °C with decomp.; ^{1}H NMR (400 MHz, $(CD_3)_2CO$, −20 °C): δ = 3.41 (brs, 8H), 3.68 (brs, 8H), 3.76–4.11 (m, 56H), 6.13 (s, 8H), 6.19 (s, 8H), 7.84 (dd, J = 8, 1 Hz, 4H), 8.13 (d, J = 1 Hz, 4H), 8.17 (d, J = 7 Hz, 8H), 8.32 (d, J = 8 Hz, 4H), 9.20 (d, J = 7 Hz, 8H); ^{13}C NMR (100 MHz, $(CD_3)_2CO$, 31 °C): δ = 65.7, 67.7, 70.7, 70.9, 71.4, 114.3, 115.5, 123.1, 125.4, 125.9, 132.1, 133.0, 135.0, 146.1, 146.3, 152.0; LSIMS: m/z = 2209 $[M - PF_6]^+$; $C_{104}H_{116}F_{24}N_4O_{22}P_4$ (2353.9): calcd C 53.07, H 4.97, N 2.38; found: C 52.87, H 5.09, N 2.12. Single crystals, suitable for X-ray crystallography, were grown by vapor diffusion of $i$$Pr_2O$ into a solution of **9**·4PF_6 in MeCN.

Cyclobis(paraquat-3,7-dibenzofuran) tetrakis(hexafluorophosphate) (10·4PF_6): A solution of **7** (36 mg, 0.10 mmol) in anhydrous DMF (1.9 mL) was added to a stirred solution of **8**·2PF_6 (81 mg, 0.10 mmol) and $FeCp_2$ (410 mg, 2.21 mmol) in anhydrous MeCN (15 mL) under N_2. After the reaction mixture had been stirred at 20 °C for 17.5 d, the solvent was removed under reduced pressure, and the residue washed by stirring with Et_2O (50 mL). The residue was worked up as described for **6**·4PF_6 to afford the title compound **10**·4PF_6 as a yellow solid (48 mg, 37%). M.p. 239 °C with decomp.; ^{1}H NMR (300 MHz, CD_3CN, 20 °C): δ = 5.94 (s, 8H), 7.43 (d, J = 1 Hz, 4H), 7.68 (dd, J = 8, 1 Hz, 4H), 8.15 (d, J = 8 Hz, 4H), 8.24 (d, J = 7 Hz, 8H), 8.93 (d, J = 7 Hz, 8H); ^{13}C NMR (75 MHz, CD_3CN, 20 °C): δ = 65.8, 112.5, 123.4, 125.6, 128.3, 128.5, 134.9, 146.4, 150.8, 157.6; LSIMS: m/z = 1135 $[M - PF_6]^+$; $C_{34}H_{26}F_{12}N_4OP_2$ (1280.7): calcd C 45.02, H 2.83, N 4.37; found C 45.73, H 2.90, N 3.83. Single crystals, suitable for X-ray analysis, were obtained when a MeCN solution of the tetracationic macrocycle was layered with $i$$Pr_2O$.

X-Ray Crystallographic Analyses: Table 4 provides a summary of the crystal data, data collection and refinement parameters for the compounds **4**-H·3PF_6, **5**·4PF_6, **6**·4PF_6, **9**·4PF_6, and **10**·4PF_6, and the complex [**4**-H·BPP34C10][PF_6]$_3$. Refinements were by full matrix least-squares based on F^2; in the case of **5**·4PF_6, the refinement was blocked on account of the large number of variable parameters. In all the structures, the major occupancy non-hydrogen atoms were refined anisotropically. All the structures, with the exception of **6**·4PF_6 and **10**·4PF_6, contain disordered PF_6^- anions. In each case, the disorder was resolved into alternate, partial occupancy orientations. All the structures contain included solvent molecules; in **10**·4PF_6, these molecules are both ordered and of full occupancy, whereas in the other five structures there is a mixture of ordered full occupancy molecules and disordered molecules distributed over multiple partial occupancy sites. All of the C–H hydrogen atoms in each of the six structures were placed in calculated positions, assigned isotropic thermal parameters, U(H) = 1.2 U_{eq}(C) [U(H) = 1.5 U_{eq}(C–Me)], and allowed to ride on their parent atoms. In **5**·4PF_6, one of the polyether linkages was found to be disordered, and alternate, partial occupancy conformations were identified. The major occupancy conformation is that illustrated. Computations were carried out with the SHELXTL PC program system.[59] The crystallographic data (excluding structure factors) for the structures reported in Table 4 have been deposited with the Cambridge Crystallographic Data Centre as supplementary publication number CCDC-100139. Copies of the data can be obtained free of charge on application to The Director, CCDC, 12 Union Road, Cambridge, CB21EZ, UK (Fax: Int. code +(1223)336-033; e-mail: deposit@chemcrys.cam.ac.uk).

Methods for the Determination of the Association Constants by UV/Vis and ^{1}H NMR Spectroscopy:

Method A: A series of solutions of the tetracationic cyclophane **6**·4PF_6 at constant concentration (1.15×10^{-3} M) and containing different amounts of BHEEN (10^{-4}–10^{-1} M) in MeCN were prepared. The absorbance at the wavelength (λ_{max}) corresponding to the maximum of the charge-transfer band for the 1:1 complex was measured for all the solutions at 25 °C. The correlation between the absorbance and the guest concentration was used[37] to evaluate the association constant (K_a) in a nonlinear curve-fitting program (Ultrafit, Biosoft, Cambridge, **1992**) running on an Apple Macintosh personal computer. A similar procedure was employed for the determination of the association constant for the [**4**-H·BPP34C10][PF_6]$_3$ complex in Me_2CO with solutions having a constant concentration of **4**-H·PF_6 and variable amounts of BPP34C10.

Method B: A series of solutions of constant concentration (2.2×10^{-3} M) of the tetracationic cyclophane **10**·4PF_6 and containing variable quantities of $FeCp_2$ (10^{-4}–10^{-1} M) in CD_3CN were prepared. The chemical shifts of the host protons attached to the bipyridinium units β to the nitrogen atoms were measured by ^{1}H NMR spectroscopy at 25 °C. The correlation between the chemical shift and the guest concentration was used[37, 38] to evaluate the association constant (K_a) in a nonlinear curve-fitting program (Ultrafit, Biosoft, Cambridge, **1992**), running on an Apple Macintosh personal computer.

Molecular Simulation: All molecular mechanics simulations (except those incorporating $FeCp_2$) were carried out by means of the Amber* forcefield as implemented in Macromodel V 5.0.[60] Sybyl molecular mechanics and AM1 and PM3 semiempirical calculations were carried out with Spartan 4.1.1.[61] All calculations were performed on a Silicon Graphics Power Indigo2 Workstation. Generally, the starting structures were assembled within the Macromodel INPUT submode and then fully minimized (final gradient <0.5 kJ Å^{-1}) by the Polak Ribiere Conjugate Gradient (PRCG) algorithm. Solvation (with extended cut-offs) was included in the form of the GB/SA solvation model for H_2O, and was utilized for all molecular mechanics simu-

Table 4. Crystal data, data collection, and refinement parameters [a].

Data	**4**-H·3PF$_6$	[**4**-H·BPP34C10][PF$_6$]$_3$	**5**·4PF$_6$	**6**·4PF$_6$	**9**·4PF$_6$	**10**·4PF$_6$
formula	$C_{34}H_{27}N_4O\cdot3PF_6$	$C_{62}H_{67}N_4O_{11}\cdot3PF_6$	$C_{76}H_{76}N_4O_{12}\cdot4PF_6$	$C_{48}H_{36}N_4O_2\cdot4PF_6$	$C_{104}H_{116}N_4O_{22}\cdot4PF_6$	$C_{48}H_{36}N_4O_2\cdot4PF_6$
solvent	$0.5\,Me_2CO\cdot0.5\,Et_2O$	2MeCN	$PhH\cdot4\,MeNO_2$	$5\,MeNO_2$	4MeCN	4MeCN
formula weight	1008.6	1561.2	2139.6	1585.9	2518.1	1444.9
color, habit	clear needles	red blocks	amber blocks	yellow prisms	red blocks	yellow plates
crystal size/mm	0.40 × 0.28 × 0.15	1.00 × 1.00 × 0.50	0.53 × 0.30 × 0.17	0.33 × 0.33 × 0.17	0.67 × 0.40 × 0.17	0.40 × 0.27 × 0.13
lattice type	triclinic	triclinic	triclinic	monoclinic	triclinic	triclinic
space group	$P\bar{1}$	$P\bar{1}$	$P\bar{1}$	$P2_1/c$	$P\bar{1}$	$P\bar{1}$
T/K	293	293	233	203	243	293
cell dimensions						
a/Å	10.848(2)	13.531(2)	10.516(2)	18.606(1)	13.606(1)	10.499(1)
b/Å	14.108(1)	14.140(2)	15.429(4)	21.884(2)	14.413(1)	12.236(1)
c/Å	16.959(2)	21.664(3)	30.595(4)	17.076(2)	17.926(2)	13.274(1)
α/deg	72.30(1)	96.08(1)	80.45(2)	–	71.80(1)	85.32(1)
β/deg	75.19(1)	95.61(2)	83.63(3)	112.47(1)	85.75(1)	72.51(1)
γ/deg	84.12(1)	111.88(2)	85.88(2)	–	64.57(1)	75.79(1)
V/Å^3	2389.6(5)	3782.3(9)	4858(2)	6425(1)	3008.6(5)	1576.6(1)
Z	2	2	2	4	1 [c]	1 [c]
D_c/g cm^{-3}	1.402	1.371	1.463	1.640	1.390	1.522
$F(000)$	1022	1612	2204	3216	1308	732
radiation used	$Cu_{K\alpha}$	$Mo_{K\alpha}$	$Cu_{K\alpha}$ [b]	$Cu_{K\alpha}$ [b]	$Cu_{K\alpha}$ [b]	$Cu_{K\alpha}$
μ/mm^{-1}	2.117	0.182	1.759	2.333	1.519	2.190
θ range /deg	4.2–60.0	1.8–22.5	1.5–55.0	2.6–60.0	2.6–60.0	3.5–63.7
no. of unique reflections						
measured	6978	9754	11886	9470	8607	5121
observed, $\lvert F_o\rvert > 4\sigma(\lvert F_o\rvert)$	5608	5985	9255	6036	5897	3904
no. of variables	633	1028	1424	929	833	426
R_1, % [d]	7.62	8.51	9.69	13.92	11.22	9.01
wR_2, % [e]	21.77	23.86	26.31	36.39	30.30	25.57
weighting factors a, b [f]	0.145, 2.943	0.154, 3.447	0.169, 9.811	0.204, 53.962	0.212, 4.827	0.160, 1.503
largest difference peak, hole /e Å^{-3}	0.75, −0.44	0.69, −0.31	0.76, −0.52	0.78, −0.60	0.90, −0.41	0.92, −0.59

[a] Details in common: graphite monochromated radiation, ω-scans, Siemens P4 diffractometer, refinement based on F^2. [b] Rotating anode source. [c] The molecule has crystallographic C_i symmetry. [d] $R_1 = \sum\lvert\lvert F_o\rvert - \lvert F_c\rvert\rvert/\sum\lvert F_o\rvert$. [e] $wR^2 = \sqrt{\{\sum[w(F_o^2 - F_c^2)^2]/\sum[w(F_o^2)^2]\}}$. [f] $w^{-1} = \sigma^2(F_o^2) + (aP)^2 + bP$.

lations that employed the Amber* forcefield. Molecular dynamics simulations (MD) were carried out at a bath temperature of 300–900 K (timestep = 1.5 fs) with data sampling during the acquisition period (generally 10–100 ps). Routinely, 100 conformations were sampled and subsequently minimized with the conditions and procedures described above. For structures containing the $FeCp_2$ unit, the general molecular mechanics forcefield Sybyl was employed. AM 1 and PM 3 semiempirical calculations were carried out on the lowest energy conformations obtained from molecular mechanics/dynamics calculations. The coordinates for $FeCp_2$ were obtained from the Daresbury Crystallographic Database.[62]

Acknowledgment: This research was supported by the Engineering and Physical Sciences Research Council (EPSRC) and the Biotechnology and Biological Sciences Research Council (BBSRC) in the UK. We also wish to acknowledge the use of the EPSRC Chemical Database Service at Daresbury (UK).

Received: October 23, 1996 [F 507]

---

[1] a) M. Mascal, *Contemp. Org. Synth.* **1994**, *1*, 31–46; b) J.-M. Lehn, *Supramolecular Chemistry*, VCH, Weinheim, **1995**; c) *Comprehensive Supramolecular Chemistry, 11 Vols* (Eds.: J. L. Atwood, J. E. D. Davies, D. D. MacNicol, F. Vögtle), Pergamon, Oxford, **1996**.

[2] Selected recent examples: a) J. A. Zerkowski, C. T. Seto, G. M. Whitesides, *J. Am. Chem. Soc.* **1992**, *114*, 5473–5475; b) P. Baxter, J.-M. Lehn, A. DeCian, J. Fischer, *Angew. Chem. Int. Ed. Engl.* **1993**, *32*, 69–72; c) S. Rüttiman, G. Bernardinelli, A. F. Williams, *ibid.* **1993**, *32*, 392–394; d) R. W. Saalfrank, R. Burak, A. Breit, D. Stalke, R. Herbst-Irmer, J. Daub, M. Porsch, E. Bill, M. Müther, A. X. Trautwein, *ibid.* **1994**, *33*, 1621–1623; e) J. Yang, J.-L. Marendez, S. J. Geib, A. D. Hamilton, *Tetrahedron Lett.* **1994**, *35*, 3665–3668; f) M. Fujita, D. Oguro, M. Miyazawa, H. Oka, K. Yamaguchi, K. Ogura, *Nature (London)* **1995**, *378*, 469–471; g) R. M. Grotzfeld, N. Branda, J. Rebek, Jr., *Science* **1996**, *271*, 487–489; h) P. R. Ashton, E. J. T. Chrystal, P. T. Glink, S. Menzer, C. Schiavo, N. Spencer, J. F. Stoddart, P. A. Tasker, A. J. P. White, D. J. Williams, *Chem. Eur. J.* **1996**, *2*, 709–728.

[3] Selected examples (not involving X-ray crystal structures): a) M. R. Ghadiri, J. R. Granja, R. A. Milligan, D. E. McRee, N. Khazanovich, *Nature (London)* **1993**, *366*, 324–327; b) F. M. Menger, S. J. Lee, *J. Am. Chem. Soc.* **1994**, *116*, 5987–5988; c) M. Kotera, J.-M. Lehn, J.-P. Vigneron, *J. Chem. Soc. Chem. Commun.* **1994**, 197–199; d) N. Kimizuka, S. Fujikawa, H. Kuwahara, T. Kunitake, A. Marsh, J.-M. Lehn, *ibid.* **1995**, 2103–2104.

[4] Wuest and coworkers have suggested that supramolecular building blocks that undergo self-assembly into organized supramolecular arrays should be termed *tectons*. See: M. Simard, D. Su, J. D. Wuest, *J. Am. Chem. Soc.* **1991**, *113*, 4696–4698. For overviews of molecular tectonics, see: a) S. Mann, *Nature (London)* **1993**, *365*, 499–505; b) J. S. Moore, *ibid.* **1995**, *374*, 495–496; c) D. Su, X. Wang, M. Simard, J. D. Wuest, *Supramol. Chem.* **1995**, *6*, 171–178.

[5] a) M. C. Etter, *Acc. Chem. Res.* **1990**, *23*, 120–126; b) C. B. Aakeroy, K. R. Seddon, *Chem. Soc. Rev.* **1993**, *22*, 397–407; c) M. J. Zaworotko, *ibid.* **1994**, *23*, 283–288; d) J. C. MacDonald, G. M. Whitesides, *Chem. Rev.* **1994**, *94*, 2383–2420; e) D. B. Amabilino, J. F. Stoddart, D. J. Williams, *Chem. Mater.* **1994**, *6*, 1159–1167; f) G. R. Desiraju, *Angew. Chem. Int. Ed. Engl.* **1995**, *34*, 2311–2327; g) *Comprehensive Supramolecular Chemistry, Vol. 6* (Eds.: J. L. Atwood, J. E. D. Davies, D. D. MacNicol, F. Vögtle), Pergamon, Oxford, **1996**.

[6] J.-M. Lehn, *Makromol. Chem. Macromol. Symp.* **1993**, *69*, 1–17.

[7] a) K. E. Drexler, *Proc. Natl. Acad. Sci. USA* **1981**, *78*, 5275–5278; b) K. E. Drexler, *Nanosystems—Molecular Machinery, Manufacturing and Computation*, Wiley, New York, **1992**; c) G. A. Ozin, *Adv. Mater.* **1992**, *4*, 612–649; d) K. E. Drexler, *Annu. Rev. Biophys. Biomol. Struct.* **1994**, *23*, 377–405.

[8] a) G. M. Whitesides, J. P. Mathias, C. T. Seto, *Science* **1991**, *254*, 1312–1319; b) J. S. Lindsey, *New J. Chem.* **1991**, *15*, 153–180; c) J.-M. Lehn, *Pure Appl. Chem.* **1994**, *66*, 1961–1966; d) D. S. Lawrence, T. Jiang, M. Levett, *Chem. Rev.* **1995**, *95*, 2229–2260; e) G. M. Whitesides, E. E. Simanek, J. P. Mathias, C. T. Seto, D. N. Chin, M. Mammen, D. M. Gordon, *Acc. Chem. Res.* **1995**, *28*, 37–44; f) D. Philp, J. F. Stoddart, *Angew. Chem. Int. Ed. Engl.* **1996**, *35*, 1154–1196.

[9] a) J. A. Zerkowski, J. C. MacDonald, C. T. Seto, D. A. Wierda, G. M. Whitesides, *J. Am. Chem. Soc.* **1994**, *116*, 2382–2391; b) S. Valiyaveettil, V. Enkelmann, K. Müllen, *J. Chem. Soc. Chem. Commun.* **1994**, 2097–2098; c) S. Hanessian, M. Simard, S. Roelens, *J. Am. Chem. Soc.* **1995**, *117*, 7630–7645; d) E. Fan, J. Yang, S. J. Geib, T. C. Stoner, M. D. Hopkins, A. D. Hamilton, *J. Chem. Soc. Chem. Commun.* **1995**, 1251–1252; e) K. Kinbara, Y. Hashimoto, M. Sukegawa, H. Nohira, K. Saigo, *J. Am. Chem. Soc.* **1996**, *118*, 3441–3449; f) K. E. Schwiebert, D. N. Chin, J. C. MacDonald, G. M. Whitesides, *ibid.* **1996**, *118*, 4018–4029; g) M. W. Hosseini, G. Brand, P. Schaeffer, R. Ruppert, A. DeCian, J. Fischer, *Tetrahedron Lett.* **1996**, *37*, 1405–1408.

0947-6539/97/0307-1148 $ 17.50+.50/0

[10] a) B. F. Abrahams, B. F. Hoskins, D. M. Michail, R. Robson, *Nature (London)* **1994**, *369*, 727–729; b) D. M. L. Goodgame, S. Menzer, A. M. Smith, D. J. Williams, *J. Chem. Soc. Chem. Commun.* **1995**, 1975–1977; c) M. Fujita, Y. J. Kwon, O. Sasaki, K. Yamaguchi, K. Ogura, *J. Am. Chem. Soc.* **1995**, *117*, 7287–7288; d) S. Subramanian, M. J. Zaworotko, *Angew. Chem. Int. Ed. Engl.* **1995**, *34*, 2127–2129; e) G. B. Gardner, D. Venkataraman, J. S. Moore, S. Lee, *Nature (London)* **1995**, *374*, 792–795; f) O. M. Yaghi, H. Li, *J. Am. Chem. Soc.* **1996**, *118*, 295–296.

[11] a) J.-Y. Ortholand, A. M. Z. Slawin, N. Spencer, J. F. Stoddart, D. J. Williams, *Angew. Chem. Int. Ed. Engl.* **1989**, *28*, 1394–1395; b) G. R. Desiraju, A. Gavezzotti, *J. Chem. Soc. Chem. Commun.* **1989**, 621–623; c) P. R. Ashton, D. Philp, N. Spencer, J. F. Stoddart, D. J. Williams, *ibid.* **1994**, 181–184; d) D. B. Amabilino, P. R. Ashton, J. F. Stoddart, S. Menzer, D. J. Williams, *ibid.* **1994**, 2475–2478; e) J. Otsuki, T. Oya, S.-H. Lee, K. Araki, *ibid.* **1995**, 2193–2194; f) R. S. Lokey, B. L. Iverson, *Nature (London)* **1995**, *375*, 303–305.

[12] a) F. H. Allen, B. S. Goud, V. J. Hoy, J. A. K. Howard, G. R. Desiraju, *J. Chem. Soc. Chem. Commun.* **1994**, 2729–2730; b) M. Mascal, J. L. Richardson, A. J. Blake, W.-S. Li, *Tetrahedron Lett.* **1996**, *37*, 3505–3506; c) V. R. Thalladi, B. S. Goud, V. J. Hoy, F. H. Allen, J. A. K. Howard, G. R. Desiraju, *Chem. Commun.* **1996**, 401–402; d) D. S. Reddy, D. C. Craig, G. R. Desiraju, *J. Am. Chem. Soc.* **1996**, *118*, 4090–4093; e) H. Bock, Z. Havlas, A. Rauschenbach, C. Näther, M. Kleine, *Chem. Commun.* **1996**, 1529–1530.

[13] For solid-state supramolecular synthesis employing both hydrogen bonding and aryl–aryl stacking interactions, see: a) J. C. Beeson, L. J. Fitzgerald, J. C. Gallucci, R. E. Gerkin, J. T. Rademacher, A. W. Czarnik, *J. Am. Chem. Soc.* **1994**, *116*, 4621–4622; b) Y. Aoyama, K. Endo, T. Anzai, Y. Yamaguchi, T. Sawaki, K. Kobayashi, N. Kanehisa, H. Hashimoto, Y. Kai, H. Masuda, *ibid.* **1996**, *118*, 5562–5571. For crystal engineering utilizing both dative bonds and hydrogen bonding, see: c) H. M. Colquhoun, J. F. Stoddart, D. J. Williams, *J. Chem. Soc. Chem. Commun.* **1981**, 849–850; d) S. B. Copp, S. Subramanian, M. J. Zaworotko, *J. Am. Chem. Soc.* **1992**, *114*, 8719–8720; e) M. M. Chowdry, D. M. P. Mingos, A. J. P. White, D. J. Williams, *Chem. Commun.* **1996**, 899–900. For solid-state supramolecular synthesis employing both hydrogen bonding and heteroatom–halogen interactions, see: f) ref. [12c]; g) D. S. Reddy, Y. E. Ovchinnikov, O. V. Shishkin, Y. T. Struchkov, G. R. Desiraju, *J. Am. Chem. Soc.* **1996**, *118*, 4085–4089. For solid state supramolecular synthesis of polymeric networks using both coordinate covalent bonds and π–π stacking interactions, see: h) J. Harrowfield, *J. Chem. Soc. Dalton Trans.* **1996**, 3165–3171; i) A. C. Deveson, S. L. Heath, C. J. Harding, A. K. Powell, *ibid.* **1996**, 3173–3178.

[14] P. R. Ashton, C. G. Claessens, W. Hayes, S. Menzer, J. F. Stoddart, D. J. Williams, *Angew. Chem. Int. Ed. Engl.* **1995**, *34*, 1862–1865.

[15] a) P. R. Ashton, S. Menzer, F. M. Raymo, G. K. H. Shimizu, J. F. Stoddart, D. J. Williams, *Chem. Commun.* **1996**, 487–490; b) F. M. Raymo, J. F. Stoddart, *Pure Appl. Chem.* **1996**, *68*, 313–322; c) M. Asakawa, P. R. Ashton, S. Menzer, F. M. Raymo, J. F. Stoddart, A. J. P. White, D. J. Williams, *Chem. Eur. J.* **1996**, *2*, 877–893.

[16] a) C. A. Hunter, *Angew. Chem. Int. Ed. Engl.* **1995**, *34*, 1079–1081; b) R. Baum, *Chem. Eng. News* **1995**, *73*(7), 37–38.

[17] For reviews, see: a) W. E. Parham in *Heterocyclic Compounds, Vol. 2* (Ed.: R. C. Elderfield), Wiley, New York, **1951**, pp. 123–144; b) M. V. Sargent, P. O. Stransky, *Adv. Heterocycl. Chem.* **1984**, *35*, 1–81.

[18] The dibenzofuran unit has been utilized previously in supramolecular chemistry. For instance, this unit has been incorporated into molecular tweezers that form complexes with 1,3,5-trinitrobenzene. See: a) M. Harmata, C. L. Barnes, *J. Am. Chem. Soc.* **1990**, *112*, 5655–5657; b) M. Harmata, C. L. Barnes, S. R. Karra, S. Elahmad, *ibid.* **1994**, *116*, 8392–8393. Furthermore, it has been used to hold peptide subunits together in order to nucleate an antiparallel β-sheet structure. See: c) H. Diaz, J. R. Espina, J. W. Kelly, *J. Am. Chem. Soc.* **1992**, *114*, 8316–8318; d) H. Diaz, K. Y. Tsang, D. Choo, J. R. Espina, J. W. Kelly, *ibid.* **1993**, *115*, 3790–3791; e) H. Diaz, K. Y. Tsang, D. Choo, J. W. Kelly, *Tetrahedron* **1993**, *49*, 3533–3545. For the incorporation of the dibenzofuran subunit into cavitands with rigidly preorganized clefts, see: f) D. J. Cram, J. M. Cram, *Container Molecules and their Guests*, The Royal Society of Chemistry, Cambridge, **1994**, pp. 102–106 and references cited therein.

[19] a) L. A. Summers, *The Bipyridinium Herbicides*, Academic Press, New York, **1980**; b) W. Sliwa, B. Bachowski, N. Zelichowicz, *Heterocycles* **1991**, *32*, 2241–2273.

[20] a) D. Philp, J. F. Stoddart, *Synlett* **1991**, 445–461; b) J. F. Stoddart, *Chem. Br.* **1991**, *27*, 714–718; c) J. A. Preece, J. F. Stoddart in *Molecular Engineering for Advanced Materials* (Eds.: J. Becher, K. Schaumberg), Kluwer Academic Publishers, Dordrecht, **1995**, pp. 1–28; d) S. J. Langford, L. Pérez-García, J. F. Stoddart, *Supramol. Chem.* **1995**, *6*, 11–27.

[21] a) G. Schill, *Catenanes, Rotaxanes, and Knots*, Academic Press, New York, **1971**; b) C. O. Dietrich-Buchecker, J.-P. Sauvage, *Chem. Rev.* **1987**, *87*, 795–810; c) J. C. Chambron, C. O. Dietrich-Buchecker, J.-P. Sauvage, *Top. Curr. Chem.* **1993**, *165*, 131–162; d) D. B. Amabilino, J. F. Stoddart, *Chem. Rev.* **1995**, *95*, 2725–2828.

[22] For reviews on template-directed synthesis, see: a) S. Anderson, H. L. Anderson, J. K. M. Sanders, *Acc. Chem. Res.* **1993**, *26*, 389–395; b) R. Hoss, F. Vögtle, *Angew. Chem. Int. Ed. Engl.* **1994**, *33*, 375–384; c) D. H. Busch, A. L. Vance, A. G. Kolchinski in *Comprehensive Supramolecular Chemistry, Vol. 9* (Eds.: J. L. Atwood, J. E. D. Davies, D. D. MacNicol, F. Vögtle), Pergamon, Oxford, **1996**, pp. 1–42.

[23] M. S. Ogii, V. I. Shcherbachenko, S. N. Petrunyan, N. K. Moshchinskaya, *Vop. Khim. Khim. Tekhnol.* **1972**, *26*, 87–95 [*Chem. Abstr.* **1973**, *78*, 84153y].

[24] W. Geuder, S. Hünig, A. Suchy, *Tetrahedron* **1986**, *42*, 1665–1677.

[25] P. L. Anelli, P. R. Ashton, R. Ballardini, V. Balzani, M. Delgado, M. T. Gandolfi, T. T. Goodnow, A. E. Kaifer, D. Philp, M. Pietraszkiewicz, L. Prodi, M. V. Reddington, A. M. Z. Slawin, N. Spencer, J. F. Stoddart, C. Vicent, D. J. Williams, *J. Am. Chem. Soc.* **1992**, *114*, 193–218 and references cited therein.

[26] BPP34C10 was synthesized by the one-pot reaction of hydroquinone with tetraethylene glycol bistosylate: a) R. C. Helgeson, T. L. Tarnowski, J. M. Timko, D. J. Cram, *J. Am. Chem. Soc.* **1977**, *99*, 6411–6418; b) H. W. Gibson, S. Liu, P. Lecavalier, C. Wu, Y. X. Shen, *ibid.* **1995**, *117*, 852–874. See also: c) Y. Delaviz, H. W. Gibson, *Polym. Commun.* **1991**, *32*, 103–105; d) Y. Delaviz, Y. X. Shen, H. W. Gibson, *Polymer* **1992**, *33*, 212–213.

[27] For other examples of heterocycle-containing catenanes, see: a) P. R. Ashton, M. A. Blower, S. Iqbal, C. H. McLean, J. F. Stoddart, M. S. Tolley, D. J. Williams, *Synlett* **1994**, 1059–1062; b) P. R. Ashton, M. A. Blower, C. H. McLean, J. F. Stoddart, M. S. Tolley, *ibid.* **1994**, 1063–1066; c) P. R. Ashton, J. A. Preece, J. F. Stoddart, M. S. Tolley, A. J. P. White, D. J. Williams, *Synthesis* **1994**, 1344–1352; d) S. Ottens-Hildebrandt, M. Nieger, K. Rissanen, J. Rouvinen, S. Meier, G. Harder, F. Vögtle, *J. Chem. Soc. Chem. Commun.* **1995**, 777–778; e) A. C. Johnston, D. A. Leigh, L. Nezhat, J. P. Smart, M. D. Deegan, *Angew. Chem. Int. Ed. Engl.* **1995**, *34*, 1212–1216; f) Z.-T. Li, P. C. Stein, J. Becher, D. Jensen, P. Mork, N. Svenstrup, *Chem. Eur. J.* **1996**, *2*, 624–633.

[28] We have recently prepared a related [2]catenane in which the 2,8-dimethyldibenzofuran units are replaced by *m,m'*-bitolyl units. See: M. Asakawa, P. R. Ashton, S. E. Boyd, C. L. Brown, S. Menzer, D. Pasini, J. F. Stoddart, M. S. Tolley, A. J. P. White, D. J. Williams, P. G. Wyatt, *Chem. Eur. J.* **1997**, *3*, 463–481.

[29] C. L. Brown, D. Philp, N. Spencer, J. F. Stoddart, *Isr. J. Chem.* **1992**, *32*, 61–67.

[30] This π-electron-rich arene has also been used for the template-directed synthesis of other tetracationic cyclophanes. See, for example: a) C. L. Brown, D. Philp, J. F. Stoddart, *Synlett* **1991**, 462–464; b) ref. [27c]; c) ref. [14]; d) P. R. Ashton, R. Ballardini, V. Balzani, A. Credi, M. T. Gandolfi, S. Menzer, L. Pérez-García, L. Prodi, J. F. Stoddart, M. Venturi, A. J. P. White, D. J. Williams, *J. Am. Chem. Soc.* **1995**, *117*, 11171–11197.

[31] R. M. Roberts, *Serendipity—Accidental Discoveries in Science*, Wiley, New York, **1989**.

[32] a) C. J. Pedersen, *J. Am. Chem. Soc.* **1967**, *89*, 7017–7036; b) C. J. Pedersen, *Angew. Chem. Int. Ed. Engl.* **1988**, *27*, 1021–1027; c) ref. [31], pp. 238–243.

[33] A. C. Johnston, D. A. Leigh, R. J. Pritchard, M. D. Deegan, *Angew. Chem. Int. Ed. Engl.* **1995**, *34*, 1209–1212.

[34] K. Weber, G. Kormany (Ciba-Geigy), *German Patent 2332089*, **1973** [*Chem. Abstr.* **1974**, *80*, 134947z].

[35] [3]Catenanes have been synthesized previously in our laboratories. See: a) P. R. Ashton, C. L. Brown, E. J. T. Chrystal, T. T. Goodnow, A. E. Kaifer, K. P. Parry, A. M. Z. Slawin, N. Spencer, J. F. Stoddart, D. J. Williams, *Angew. Chem. Int. Ed. Engl.* **1991**, *30*, 1039–1042; b) D. B. Amabilino, P. R. Ashton, C. L. Brown, E. Córdova, L. A. Godínez, T. T. Goodnow, A. E. Kaifer, S. P. Newton, M. Pietraszkiewicz, D. Philp, F. M. Raymo, A. S. Reder, M. T. Rutland, A. M. Z. Slawin, N. Spencer, J. F. Stoddart, D. J. Williams, *J. Am. Chem. Soc.* **1995**, *117*, 1271–1293.

[36] For the recent synthesis of a [3]catenate, incorporating Cu^I ions, by another group, see: J.-M. Kern, J.-P. Sauvage, J.-L. Weidmann, *Tetrahedron* **1996**, *52*, 10921–10934.

[37] K. A. Connors, *Binding Constants*, Wiley, New York, **1987**.

[38] T. Wang, J. S. Bradshaw, R. M. Izatt, *J. Heterocycl. Chem.* **1994**, *31*, 1097–1114.

[39] A pseudorotaxane is an interwoven inclusion complex in which a molecular "thread" is encircled by one or more macrorings in such a way that the extremities of the thread are projected away from the center of the ring; not all of these extremities possess bulky "stopper" groups, so that the pseudorotaxane's components are free to dissociate into separate molecular species, that is, as distinct from rotaxanes, there is no mechanical bond present to hold the system together. See: a) P. R. Ashton, D. Philp, N. Spencer, J. F. Stoddart, *J. Chem. Soc. Chem. Commun.* **1991**, 1677–1679; b) D. B. Amabilino, I. W. Parsons, J. F. Stoddart, *Trends Polym. Sci.* **1994**, *2*, 146–152; c) P. R. Ashton, P. J. Campbell, E. J. T. Chrystal, P. T. Glink, S. Menzer, D. Philp, N. Spencer, J. F. Stoddart, P. A. Tasker, D. J. Williams, *Angew. Chem. Int. Ed. Engl.* **1995**, *34*, 1865–1869; d) ref. [21d]; e) ref. [2h].

[40] P. R. Ashton, D. Philp, M. V. Reddington, A. M. Z. Slawin, N. Spencer, J. F. Stoddart, D. J. Williams, *J. Chem. Soc. Chem. Commun.* **1991**, 1680–1683.

[41] For an example of a system that undergoes slow complexation and decomplexation on the ^1H NMR timescale, and therefore displays resonances for both complexed and uncomplexed species, see: a) ref. [39c]; b) P. T. Glink, C. Schiavo, J. F. Stoddart, D. J. Williams, *Chem. Commun.* **1996**, 1483–1490; c) ref. [2h].

[42] a) H. M. Colquhoun, J. F. Stoddart, D. J. Williams, *Angew. Chem. Int. Ed. Engl.* **1986**, *25*, 487–507; b) S. J. Loeb in *Comprehensive Supramolecular Chemistry, Vol. 1* (Eds.: J. L. Atwood, J. E. D. Davies, D. D. MacNicol, F. Vögtle), Pergamon, Oxford, **1996**, pp. 733–753; c) F. M. Raymo, J. F. Stoddart, *Chem. Ber.* **1996**, *129*, 981–990.

[43] The kinetic and thermodynamic data were calculated by two procedures: a) the *coalescence method*, where values for the rate constant k_c at the coalescence temperature (T_c) were calculated (I. O. Sutherland, *Annu. Rep. NMR Spectrosc.* **1971**, *4*, 71–235) from the approximate expression $k_c = \pi(\Delta\nu)/(2)^{1/2}$, where $\Delta\nu$ is the limiting chemical shift difference (Hz) between the coalescing signals in the absence of exchange; b) the *exchange method*, where values of k_{ex} were calculated (J. Sandström, *Dynamic NMR Spectroscopy*, Academic Press, London, **1982**, Ch. 6) from the approximate expression $k_{ex} = \pi(\Delta\nu)$, where $\Delta\nu$ is the difference (Hz) between the line width at a temperature T_{ex}, where exchange of sites is taking place, and the line width in the absence of exchange. The Eyring equation was subsequently employed to calculate $\Delta G_c^{\ddagger}$ or $\Delta G_{ex}^{\ddagger}$ values at T_c or T_{ex}, respectively.

[44] The dynamic processes occurring in catenanes of this type have been discussed previously in several publications. For instance, see: a) ref. [8f]; b) ref. [21d]; c) ref. [25]; d) ref. [35b].

[45] This terminology has recently been introduced by Desiraju to indicate identifiable design elements in supramolecular synthesis. See ref. [5f] for details.

[46] a) M. Fujita in *Comprehensive Supramolecular Chemistry, Vol. 9* (Eds.: J. L. Atwood, J. E. D. Davies, D. D. MacNicol, F. Vögtle), Pergamon, Oxford, **1996**, pp. 254–262; b) W. Hayes, J. F. Stoddart in *Large Ring Molecules* (Ed.: J. A. Semlyn), Wiley, New York, **1996**, pp. 433–471 and references cited therein.

[47] For a similar example where a two-component supramolecular macrocycle is formed in the solid state by virtue of [N···H] hydrogen bonding, see: K. Tanaka, Y. Kitahara, H. Suzuki, H. Osuga, Y. Kawai, *Tetrahedron Lett.* **1996**, *37*, 5925–5928.

[48] The crossed aryl–aryl stacking of dibenzofuran systems, where two of these units are oriented in an antiparallel manner with respect to one another, has been noted previously: a) O. Dideberg, L. Dupont, J. M. André, *Acta Crystallogr. Sect. B* **1972**, *28*, 1002–1007; b) A. Banerjee, *ibid.* **1973**, *29*, 2070–2074; c) C. R. Hubbard, A. D. Mighell, I. H. Pomerantz, *ibid.* **1978**, *34*, 2381–2384.

[49] Red blocks suitable for crystallographic analysis were obtained when an MeCN solution containing equimolar quantities of 4-H·3PF$_6$ and BPP34C10 was layered with Et$_2$O.

[50] a) F. M. Raymo, J. F. Stoddart, *Trends Polym. Sci.* **1996**, *4*, 208–211; b) M. Asakawa, P. R. Ashton, G. R. Brown, W. Hayes, S. Menzer, J. F. Stoddart, A. J. P. White, D. J. Williams, *Adv. Mater.* **1996**, *8*, 37–41; c) P. R. Ashton, R. Ballardini, V. Balzani, M. Belohradsky, M. T. Gandolfi, D. Philp, L. Prodi, F. M. Raymo, M. V. Reddington, N. Spencer, J. F. Stoddart, M. Venturi, D. J. Williams, *J. Am. Chem. Soc.* **1996**, *118*, 4931–4951.

[51] Analogously, pyrazine perchlorate shows the formation of a linear tape in the solid state: T. Glowiak, L. Sobczyk, E. Grech, *Chem. Phys. Lett.* **1975**, *34*, 292–293.

[52] For a noteable example where the optical purity of a tecton dictates the type of superstructure formed, see: M.-J. Brienne, J. Gabard, M. Leclerq, J.-M. Lehn, M. Cesario, C. Pascard, M. Chevé, G. Dutruc-Rosset, *Tetrahedron Lett.* **1994**, *35*, 8157–8160.

[53] For other examples of the formation of nanotubular structures from macrocyclic species in the solid state, see: a) B. Odell, M. V. Reddington, A. M. Z. Slawin, N. Spencer, J. F. Stoddart, D. J. Williams, *Angew. Chem. Int. Ed. Engl.* **1988**, *27*, 1547–1550; b) P. J. Stang, K. Chen, A. M. Arif, *J. Am. Chem. Soc.* **1995**, *117*, 8793–8797; c) ref. [14]; d) J. D. Hartgerink, J. R. Granja, R. A. Milligan, M. R. Ghadiri, *ibid.* **1996**, *118*, 43–50; e) P. R. Ashton, C. L. Brown, S. Menzer, S. A. Nepogodiev, J. F. Stoddart, D. J. Williams, *Chem. Eur. J.* **1996**, *2*, 580–591.

[54] Examination of this structure both by molecular dynamics/mechanics and by AM1 and PM3 semiempirical energy calculations, predict that this conformational isomer is some 4 kcal mol^{-1} lower in energy than its *anti* congener. This energy difference presumably arises as a consequence of an accumulation of subtle noncovalent interactions present in the *syn* conformer which would not be present in the *anti* conformer. This leads to a definite preference, at least in the solid state, for the observed conformation. Interestingly, analysis of the energies of both the *syn* and *anti* conformers of the uncatenated tetracationic cyclophane **6**$^{4+}$, both at the molecular mechanics (Amber*) and semiempirical (PM3 and AM1) level, reveal no significant energy differences between the two geometries, suggesting that the observation of only the *anti* conformation in the solid state (Figure 7) probably arises as a consequence of favorable packing interactions and not as a function of an inherent energy difference between the two conformers.

[55] Previously, we have observed only outward bowing of the bipyridinium units in [2]catenanes of this kind. For instance, see: a) ref. [25]; b) D. B. Amabilino, P. R. Ashton, M. S. Tolley, J. F. Stoddart, D. J. Williams, *Angew. Chem. Int. Ed. Engl.* **1993**, *32*, 1297–1301; c) ref. [28].

[56] W. C. Still, M. Kahn, A. Mitra, *J. Org. Chem.* **1978**, *43*, 2923–2925.

[57] P. G. Jones, *Chem. Br.* **1981**, *17*, 222–225.

[58] S. von Niementowski, *Chem. Ber.* **1901**, *34*, 3325–3337.

[59] SHELXTL PC version 5.03, Siemens Analytical X-Ray Instruments, Madison, WI, **1994**.

[60] Macromodel V 5.0: F. Mohamadi, N. G. J. Richards, W. C. Guida, R. Liskamp, M. Lipton, C. Caufield, G. Chang, T. Hendrickson, W. C. Still, *J. Comput. Chem.* **1990**, *11*, 440–467.

[61] Spartan V 4.1, Wavefunction, 18401 Von Karman Ave., 370 Irvine CA 92715.

[62] a) D. A. Fletcher, R. F. McMeeking, D. Parkin, *J. Chem. Inf. Comput. Sci.* **1996**, *36*, 746–749; b) F. H. Allen, O. Kennard, *Chemical Design Automation News* **1993**, *8*(1), *1*, 31–37.